Universidade de Lisboa

Faculty of Sciences
Department of Physics

Wetting of cholesteric liquid crystals

Maria Carolina Figueirinhas Pereira

Master's thesis

Master in Physics

Condensed Matter Physics and Nanomaterials

2015

Universidade de Lisboa

Faculty of Sciences
Department of Physics

Wetting of cholesteric liquid crystals

Maria Carolina Figueirinhas Pereira

Master's thesis

Advised by Prof. Dr. Margarida Telo da Gama
and Co-Advised by Dr. Nelson Rei Bernardino

Master in Physics

Condensed Matter Physics and Nanomaterials

2015

Contents

List of Figures

Acknowledgments

A number of people were very important to the writing of this thesis, directly or indirectly.

I would like to start by expressing my sincere gratitude to my co-adviser Dr. Nelson R. Bernardino, without whom this thesis would not have been possible.

I would also like to give special thanks to my advisor Prof. Dr. Margarida Telo da Gamma who contributed to my physics formation and never ceased to give me advice on my academic choices, not only throughout the project but also throughout both my Degree and Master's.

I thank all the people involved in this projects who have contributed to this thesis with many helpful discussions and suggestions. Special thanks is due to Dr. Nuno M. Silvestre, who crucially helped me with the computational program and software.

I also thank my friends and family for their unfailing support.

Financial support from Fundação para a Ciência e a Tecnologia (FCT) under grants PTDC/FIS/119162/2010, PEstOE/FIS/UI0618/2014, SFRH/BPD/63183/2009, and EXCEL/FIS-NAN/0083/2012 is thankfully acknowledged.

Abstract

Recently, wetting phenomena in cholesteric systems have started to receive increasing attention. The Landau-de Gennes formalism has proved ideal for the development of a theoretical understanding of the underlying physics of Liquid Crystals (LCs). In this thesis, we take advantage of this formalism to model a free interface between a cholesteric and an isotropic phase and the wetting of a substrate by a cholesteric LC. For simple cholesteric systems it's easy to build an analytic model but for situations where the system is elastically distorted we need to rely on numerical models.

In this thesis we begin with a brief overview of theoretical approaches used when describing wetting by simple fluids and by liquid crystals. We present the phenomenological Landau-de Gennes (LdG) free energy model as well as the main results known for wetting in nematics and interfacial phenomena in cholesterics. We are concerned with the thermodynamic properties of the cholesteric system and, therefore, we analyze equilibrium configurations obtained by minimizing the LdG free energy. Theory predicts that a nematic and a non-distorted cholesteric have the same wetting properties. The numerical study of the properties of the interface shows the formation of topological defects for distorted cholesterics along with a relaxation of the interface to an undulated pattern whose profile is set by the intrinsic properties of the LC. The surface tension (σ) of the interface and the anchoring strength of the LC molecules at the substrate for which the wetting transition occurs (ω^t) are found to reach the nematic limit when the cholesteric periodicity is very large. For small periodicity and certain values of the elastic constants the cholesteric phase may become unstable giving place to more stable blue phases. Finally we see that ω^t follows the behavior of σ, meaning that the surface tension drives the wetting transition.

Keywords: Cholesteric, Landau-de Gennes Model, Surface Tension, Interfacial Phenomena, Anchoring Strength, Wetting

Resumo

Desde a descoberta dos Cristais Líquidos (CLs), que a busca por aplicações destes materiais com propriedades mecânicas e electro-ópticas tão peculiares tem sido uma área de grande interesse. As suas aplicações mais conhecidas incluem aplicações à medicina – CLs podem ser usados como termómetros – e à fotónica – CLs estão na base dos LCDs (*Liquid Crystal Displays*) que representam cerca de 90% do mercado mundial de dispositivos de visualização.

Tal como os LCDs, o fenómeno de molhagem tem sido alvo de grande estudo, uma vez que diversos fenómenos de molhagem são parte integrante do nosso dia-a-dia. Em particular, o estudo da molhagem engloba o estudo de fenómenos interfaciais, cuja compreensão ajuda a responder a questões fundamentais tais como definir uma interface e calcular uma tensão de superfície.

Recentemente, o problema da molhagem por colestéricos começou a atrair atenções, não só pelas potenciais aplicações tecnológicas mas também pelo facto de ser um sistema ainda pouco explorado. O formalismo de *Landau-de Gennes* (LdG) tem-se provado ideal para o desenvolvimento de um entendimento teórico da física subjacente aos sistemas de CLs. Nesta dissertação, tiramos partido deste formalismo para modelar uma interface CI livre (interface entre uma fase líquido-cristalina colestérica e uma isotrópica) e a molhagem de uma superfície plana por um colestérico (interface CI na presença de uma superfície). Para sistemas simples de colestéricos é fácil deduzir um modelo analítico mas para situações mais complexas, onde o sistema apresenta distorções elásticas, precisamos de recorrer a modelos numéricos.

Na presente dissertação começamos por introduzir o fenómeno de molhagem para fluidos simples. A equação de *Young* estabelece a condição de molhagem quando o ângulo de contacto é zero. Com o intuito de introduzir a molhagem por CLs, fazemos um resumo das propriedades dos CLs, assim como da descrição mesoscópica fenomenológica que irá ser usada para modelar cristais líquidos colestéricos – o modelo da energia livre de *Landau-de Gennes*. Para temperaturas menores do que uma temperatura crítica, os CLs exibem uma fase onde as moléculas apresentam um certo nível de ordenamento médio (fase ordenada). Acima dessa temperatura crítica, os CLs comportam-se como fluidos isotrópicos (fase isotrópica). Devido à simetria dos CLs, o parâmetro de ordem que caracteriza a fase líquido-cristalina ordenada é um tensor de segunda ordem. O modelo de energia livre de LdG descreve o CL em termos de duas densidades de energia livre: uma que decreve a transição entre a fase líquido-cristalina e a fase isotrópica, e uma que penaliza variações do parâmetro de ordem, i.e., penaliza distorções elásticas. Introduzimos também a densidade de energia livre associada à superfície plana que penaliza desvios da

orientação molecular em relação à orientação favorecida na superfície. O conceito de defeitos topológicos em CLs é desenvolvido mencionando os dois tipos de defeitos existentes em colestéricos: pontos e linhas (*disclinações*). De seguida, os resultados da literatura mais importantes para a molhagem por CLs nemáticos e para os fenómenos interfaciais em colestéricos são revistos. Quando uma surperfíe plana é molhada por um nemático, a interface nemático-isotrópico é sempre plana. Para colestéricos isto pode já não ser verdade uma vez que um colestérico forma defeitos topológicos perto da interface CI para quase todas as configurações colestéricas. A única interface CI livre que não exibe defeitos topológicos corresponde a um colestérico com camadas paralelas à interface onde o ancoramento preferencial é também paralelo à interface. Estudos experimentais mostram a formação destes defeitos topológicos perto da interface CI quando uma superfície é molhada por um colestérico. Estes defeitos apresentam ainda uma dinâmica peculiar à medida que o filme de colestérico cresce na superfície.

Neste trabalho, estamos interessados no estudo das propriedades termodinâmicas de sistemas colestéricos e, como tal, analisamos configurações de equilíbrio obtidas pela minimização da energia livre LdG. Segundo os cálculos teóricos realizados para o estudo da molhagem por um colestérico sem distorções elásticas, tal colestérico exibe as mesmas propriedades de molhagem que um nemático. Para o estudo de sistemas colestéricos com distorções elásticas tivemos de recorrer a Métodos de Elementos Finitos para a minimização numérica da energia livre LdG. O estudo numérico das propriedades da interface CI mostra que há formação de disclinações perto da interface o que leva a interface a relaxar para uma interface ondulada de modo a evitar a formação de mais disclinações de elevado custo energético. O perfil da interface ondulada é determinado pelas propriedades intrínsecas do colestérico: a periodicidade (*pitch* P) e a razão κ entre as constantes elásticas L_1 e L_2 do sistema ($\kappa = L_2/L_1$). A amplitude das ondulações escala de acordo com $A \sim \sqrt{P}$ e $A \sim k$, contrariamente ao que é sugerido na literatura. Esta diferença deve-se à presença de duas escalas de comprimento no sistema: a escala do *pitch* P e do comprimento de correlação ξ, que determina o tamanho do núcleo dos defeitos topológicos. Apesar de $\xi << P$, a influência de ξ é ainda notória uma vez que a interface ondula para evitar a formação de mais defeitos topológicos.

Do ponto de vista termodinâmico, as distorções elásticas e os defeitos topológicos fazem parte da interface. A energia livre da interface inclui, portanto, a energia das distorções e defeitos. Sendo a tensão de superfície a energia livre por unidade de área, torna-se simples determinar a tensão de superfície da interface CI em função P e κ. Para elevados valores de P, a tensão de superfície tende para o valor assimptótico (limite do nemático), conforme esperado. Para pequenos valores de P, a tensão de superfície diminui com a diminuição do valor de κ chegando mesmo a assumir valores negativos. Isto indica que nesta região de parâmetros a fase colestérica deixa de ser a fase mais estável dando lugar a fases mais exóticas como as *blue phases*. Estas fases são caracterizadas pela formação

de regiões de *double-twist* que têm energia inferior à de uma phase colestérica.

No que toca ao estudo da molhagem por colestéricos, neste trabalho estamos interessados no estudo da molhagem de uma superfície plana induzida pelo aumento da força do ancoramento favorecido na superfície. Se considerarmos um cholestérico na fase isotrópica em contacto com uma superfície plana à temperatura the coexistência colestérico-isotrópico, há medida que a força do ancoramento imposto na superfície aumenta, começa a ser favorável ordenar as moléculas perto da superfície formando-se um filme the fase colestérica ordenada. A espessura do filme cresce com o aumento da força do ancoramento até a distância entre a superfície plana e a interface CI ser grande em relação ao tamanho do sistema. Neste ponto ocorre a transição de molhagem. Ao valor da força do ancoramento para o qual se dá a transição de molhagem dá-se o nome de constante de ancoramento de transição ω^t. Para o caso em que o filme colestérico não exibe distorções elásticas ou defeitos, ω^t é independente do valor the P, confirmando o resultado de um colestérico e um nemático uniformes terem as mesmas propriedades de molhagem. Na situação em que a fase ordenada exibe distorções ou defeitos, ω^t tende para o limite do nematico para grandes valores de P, tal como esperado, sendo a ligeira diferença entre os valores devido às distorções e defeitos adicionais que não estão presentes no nemático. Para pequenos valores de P, ω^t diminui com a diminuição de κ, tal como σ, o que sugere a emergência de *blue phases*. De facto, ω^t segue a variação de σ ou, por outras palavras, a tensão de superfície "controla" a transição de molhagem.

Palavras-chave: Colestérico, Modelo Landau-de Gennes, Tensão de Superfície, Fenómenos Interfaciais, Força de Ancoramento, Molhagem

Chapter 1

Introduction

Wetting phenomena are widespread in nature and occur whenever a surface is exposed to an environment [1]. The water flux on roads, the deposition of fertilizers' aqueous solutions on hydrophobic leaves and the formation of the hydrolipidic film - film composed out of water and lipids that coats and protects the human skin - are examples that depend on the wetting properties of the fluids on those substrates [2]. Understanding why and when a liquid wets a surface helps us to improve our knowledge of everyday events as well as design new materials. Furthermore, the study of interfacial and wetting phenomena helps us answer fundamental questions such as how to define an interface and calculate a surface tension.

Let's then start by introducing the key concept which allows us to describe wetting phenomena – the concept of interface. One can see an interface as the region that separates two different phases, as depicted in Fig. 1.1. In the case of simple fluids, like water, the different phases are characterized by a well defined value of the density ρ. At the interface ρ varies continuously from one value to another. Thus, near an interface, one

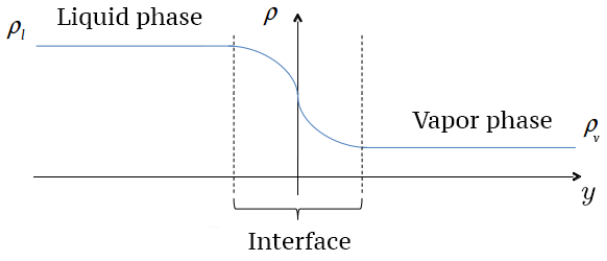

Figure 1.1: Schematic representation of the density profile of the liquid-vapor interface and of the uniform liquid and vapor phases. The density ρ assumes constant values ρ_l and ρ_v at the uniform bulk liquid and vapor phases, respectively. In this representation the y-axis indicates the direction perpendicular to the liquid-vapor interface.

can distinguish three free energies. The free energies of both phases (bulk free energy) and the free energy of the interface that takes into account the variation of ρ. The free energy of the interface per unit area, σ, is called *surface tension*.

Knowing this, wetting phenomena are summed up by Young's equation, which gives the relation between the surface tensions of the intervening interfaces in the situation described in Fig. 1.2 [3, 4]: When considering a liquid drop in contact with a planar

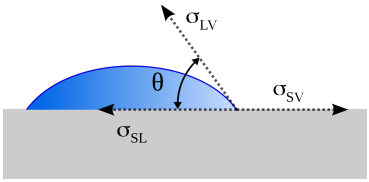

Figure 1.2: Macroscopic view of the contact angle θ and its relation with the surface tensions σ_{sl}, σ_{sv} and σ_{lv} of the solid-liquid, solid-vapor and liquid-vapor interfaces, respectively. Adapted from `en.wikipedia.org/wiki/Contact_angle`.

substrate, three different phases are present – solid, liquid and vapor phase – and thus the equilibrium state results from an interplay between the properties of three interfaces, and the corresponding surface tensions. Young's equation gives the relation between these three surface tensions σ_{sl}, σ_{sv} and σ_{lv} of the solid-liquid, solid-vapor and liquid-vapor interfaces, respectively, and the contact angle θ, the angle at which the liquid-vapor interface meets the solid phase, measured in the liquid phase:

$$\sigma_{sv} - \sigma_{sl} = \sigma_{lv} \cos(\theta). \tag{1.1}$$

The substrate is said to be dry when $\theta = 180^{\circ}$. The equilibrium state corresponds to a perfect spherical drop of the liquid phase in contact through just one point with the solid phase. One has partial wetting of the substrate when $0^{\circ} < \theta < 180^{\circ}$, which corresponds to an equilibrium state where the contact area between the liquid and solid phases is finite. There is complete wetting of the substrate when $\theta = 0^{\circ}$ and in this case the liquid spreads out forming a thin liquid film on the substrate. The transition from a partial wetting state to a complete wetting state is called wetting transition [2]. For complete wetting Young's equation becomes

$$\sigma_{sv} - \sigma_{sl} = \sigma_{lv} \Leftrightarrow \sigma_{sv} = \sigma_{sl} + \sigma_{lv}. \tag{1.2}$$

This condition is also known as Antonow's rule [3].

The wetting problem has been studied regarding not only simple but also complex fluids, such as liquid crystals (LC). Due to their mechanic and electro-optic properties, liquid crystals have played a considerable role in several fields like medicine – LCs are used as thermometers – and photonics – LCs are the base of LCDs (Liquid Crystal Displays) which in turn represent around 90% of the world display market.

Liquid crystals are oily materials composed by particles/molecules that have anisotropic shape (e.g. are elongated). LCs have several phases: the isotropic phase that behaves like

a simple fluid and the liquid crystalline phases (see Fig. 1.3). For a certain temperature

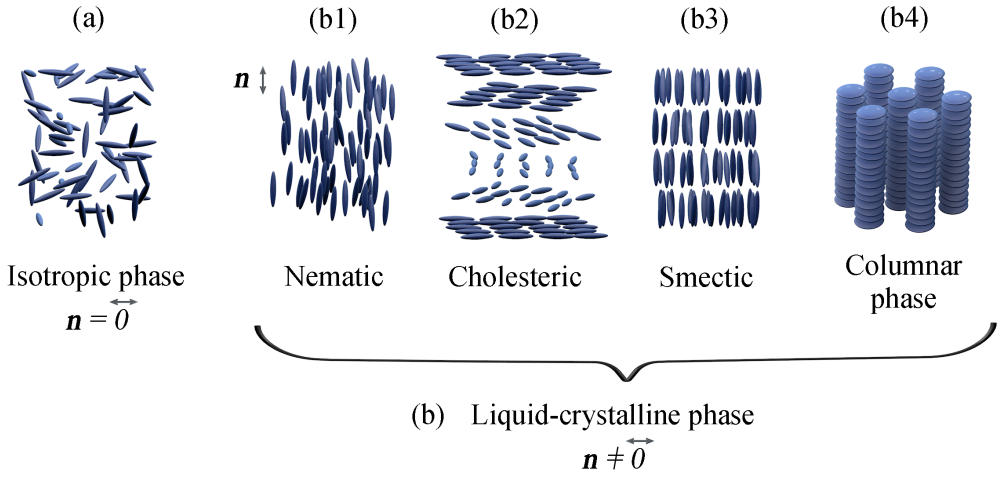

Figure 1.3: Representation of the local molecular ordering and the director for the different LC phases: (a) isotropic phase and (b) liquid crystalline phases – (b1) nematic, (b2) cholesteric, (b3) smectic and (b4) columnar phase.

or particle concentration, LCs self-organize and develop the liquid crystalline phase which is a mesophase between the liquid and solid phase. Hence the name *liquid crystal*. The liquid crystalline phase is characterized by orientational and partial positional ordering of the constituent molecules. The average orientation of the molecules defines the director $\mathbf{n}$, with the directions $\mathbf{n}$ and $-\mathbf{n}$ being equivalent. The least ordered liquid crystalline phase is the *nematic* (Fig. 1.3(b1)) where there is only long-range orientational order of the molecules. If the molecules exhibit chirality, one has a chiral nematic, usually known as *cholesteric*, where the director describes a helix in space (Fig. 1.3(b2)). When there is positional ordering of the molecules in one dimension, the mesophase is called *smectic* where the molecules are ordered in layers (Fig. 1.3(b3)). For positional ordering in two dimension, one has the *columnar phase* where the molecules are ordered in columns (Fig. 1.3(b4)) [5]. The long-range orientational order of the particles/molecules is the main characteristic that makes LCs unique comparatively, for example, to solids: it can propagate from nm to μm and it is responsive to external fields. When a LC is under confinement, the orientation of the molecules at the confining boundaries (substrates or interfaces) can conflict with the natural orientational order leading to the formation of equilibrium configurations with regions where the orientation of the molecules is undefined. These regions are called *topological defects*. In a nematic LC, the topological defects can either be points or lines.

While in the problem of wetting by simple fluids one has a substrate, a liquid, and a vapor phase, one of the interesting aspects in the study of the wetting by LCs is to consider a substrate, a liquid crystalline phase and its isotropic phase. The isotropic-liquid

crystalline interface is the region where the order of the molecules varies from the value at the bulk liquid crystalline phase to zero at the isotropic phase. A substrate is said to be dry if it is in contact with the isotropic phase. When a substrate imposes a preferential orientation of the molecules, it breaks the symmetry of the LC [6]. So, when a LC in the isotropic phase, at the isotropic-liquid crystalline phase coexistence temperature, is in contact with a substrate a thin liquid crystalline film forms near the surface. At this point, the substrate is said to be partially wet. By further increasing the strength of the imposed preferential orientation of the molecules at the substrate, the film thickens and when its thickness reaches macroscopic dimensions one has the complete wetting of the substrate by the ordered phase. Note that previously we explained the wetting transition through the Young's equation. That is a macroscopic description of the wetting phenomenon. In the microscopic point of view, the substrate is only completely wet when the distance between the substrate and the liquid-vapor/isotropic-liquid crystalline phase interface is very large.

Recent experiments on the wetting of a planar surface by a cholesteric show very interesting phenomena like the formation of a striped pattern at the isotropic-cholesteric interface (see Fig. 1.4) [6]. The stripped pattern is due to the formation of disclination

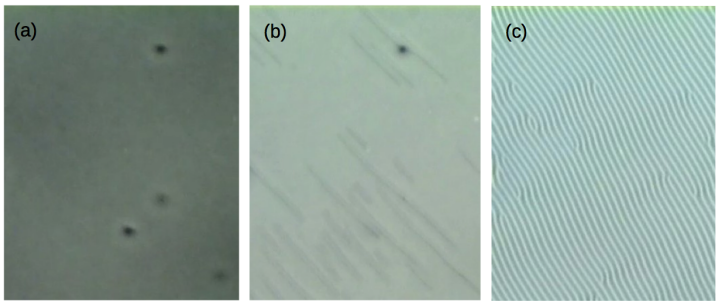

Figure 1.4: Formation of disclination lines at the cholesteric-isotropic interface, as the temperature is lowered ((a) → (b) → (c)). Adapted from [6].

lines (topological line defects). These defects confer a complex behavior to the interface. Theoretical studies claim that under certain conditions the isotropic-cholesteric interface acquires a waved pattern in order to avoid the formation of additional topological defects which have a big energetic cost. This pattern depends on both the temperature and the dopant concentration [1] [7]. Understanding the formation and the properties of this structured interface allows the application of cholesterics as substrates with tunable structure. These cholesteric substrates can in turn potentially be used for assisted self-assembly of nanoparticles [8].

In this thesis we are particularly interested in studying the wetting of surfaces by cholesterics in order to understand the complex behavior of the isotropic-cholesteric in-

[1] A cholesteric (chiral nematic) is obtained from a nematic by adding a dopant. The bigger the dopant concentration, the bigger the chirality of the liquid crystal

terface observed in the experiments in the wetting context [6]. Furthermore, from a fundamental point of view, this work extends the study of the already known wetting by simple fluids and nematics. Also, the wetting of a substrate by a cholesteric is an example of a confined cholesteric system. Cholesterics have been studied under confined geometries like drops [9] but the behavior of a cholesteric confined between a substrate and an interface is still poorly understood.

Liquid crystals have been modeled using molecular and phenomenological approaches depending on the size and typical scale of the systems. In this thesis we are interested in the study of the wetting phenomenon in cholesteric systems from the microscopic point of view but we are not interested in a molecular description of the system. We want to study thermodynamically stable configurations. Thus, we will adopt a phenomenological mean field description based on the free energy expansion in terms of a mesoscopic order parameter. In general, all the models have only a few analytical solutions, so we will rely on numerical methods – minimization of the free energy through a finite element method – to perform the necessary calculations.

In the next Chapter, we start by introducing wetting phenomena in simple fluid systems. Then we review the phenomenological Landau-de Gennes free energy model, as well as the surface anchoring and topological defects. The main results in the literature known for wetting in nematics and interfacial phenomena in cholesterics are also reviewed. In Chapter 3 we present the theoretical predictions for the reduced temperature and for the transition anchoring constant as functions of P and κ, for the non-distorted cholesteric. In chapter 4 the numerical model of a cholesteric is presented, as well as the numerical technique for the free energy minimization. Chapter 5 is devoted to the numerical study of the CI interface's properties and Chapter 6 is concerned with the numerical findings of a cholesteric wetting a planar surface that imposes parallel anchoring of the LC molecules. The concluding Chapter 7 summarizes the main results and findings presented in this thesis.

Chapter 2

Theoretical Background

In this Chapter we present the theoretical approaches used when describing wetting by simple fluids and by liquid crystals. We also present the phenomenological mesoscopic description that will be further used to model the cholesteric liquid crystal – the Landau-de Gennes free energy model.

2.1 Wetting of surfaces by isotropic fluids

The basic description of wetting phenomena was already introduced in the previous Chapter using a **macroscopic description**. The macroscopic description is given in terms of the *contact angle*, θ, whose value is set by the properties of the intervening interfaces – the surface tension. The relation between the surface tensions and θ is given by Young's equation (Eq. 1.1).

When the liquid phase is water, depending on the properties of the substrate, one can observe two different phenomena – hydrophobicity and hydrophilicity (Fig. 2.1). The

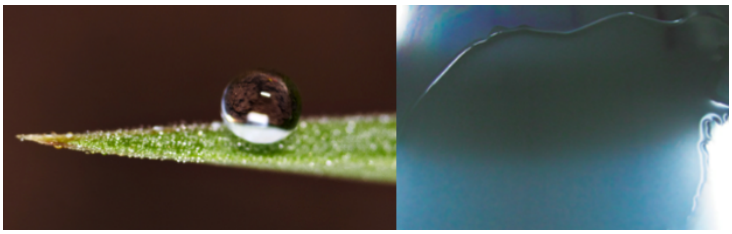

Figure 2.1: Examples of water on hydrophobic (left) and hydrophilic (right) surfaces. (left) Sphere-like water drop on a hydrophobic surface. (right) Water film spread on a hydrophilic surface. Adapted from `en.wikipedia.org/wiki/Hydrophobe` and `www.durabilityanddesign.com/news/?fuseaction=view&id=5571`.

substrate is said to be hydrophobic if it repels the water. In this case, the water acquires a drop-like shape. In terms of the contact angle, one has a hydrophobic substrate when $90^o < \theta \leq 180^o$. If the substrate has affinity with water, it is called hydrophilic. In the

lowest energy state the water spreads on the substrate. In terms of the contact angle the substrate is hydrophilic if $0^o \leq \theta \leq 90^o$.

The **microscopic description** is easily understood if one considers a vapor, at the liquid-vapor coexistence temperature, in contact with a wettable substrate. In this situation the substrate is said to be dry. As the pressure is raised, a thin film of the liquid phase forms near the substrate and the substrate becomes partially wet. For higher pressure values, the liquid film grows and the complete wetting occurs when the distance between the substrate and the liquid-vapor interface becomes very large.

Theoretically, there's complete wetting of the substrate when this distance goes to infinity. This microscopic point of view allows the theoretical determination of the surface tension. For a simple fluid with a density profile like the one in Fig. 2.2, the surface

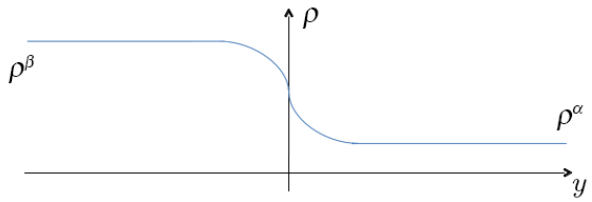

Figure 2.2: Schematic representation of the density profile of a simple fluid interface. The density profile follows approximately a hyperbolic tangent, going from a high dense phase value ρ^β to a less dense phase value ρ^α along the direction perpendicular to the interface (given by the y-axis).

tension of a free equilibrium interface between two coexistent phases is determined by simply performing the integral

$$\sigma = \int_{-\infty}^{+\infty} \Psi(y) dy, \tag{2.1}$$

where the y-axis gives the direction perpendicular to the interface and Ψ is the excess free energy density. Following the Landau theory, $\Psi(y)$ can be approximated to an expansion in power series in the density $\rho(y)$ and its derivatives $\rho'(y)$

$$\begin{aligned} \Psi(y) &= \tilde{g}(\rho(y)) + \frac{1}{2} m (\rho'(y))^2 \\ \tilde{g}(\rho) &= g(\rho) - g_0. \end{aligned} \tag{2.2}$$

$g(\rho)$ is the usual Gibbs free energy density that at the coexistence temperature of the two phases has a shape like the one in Fig. 2.3. g_0 is the Gibbs free energy density of the two coexistent bulk phases so that $\tilde{g}(\rho^\alpha) = \tilde{g}(\rho^\beta) = 0$.

The density profile that minimizes the surface tension is determined by solving the Euler-Lagrange equation that results from the minimization of the functional $\sigma[\rho(y), \rho'(y)]$ using a variational principle. Once the density profile is known, one can finally calculate σ.

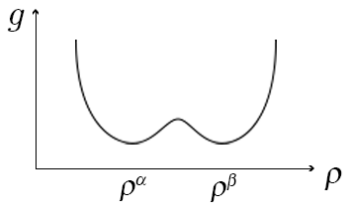

Figure 2.3: Sketch of the Gibbs free energy of a simple fluid at the low dense-high dense phase coexistence temperature. The equilibrium phases with densities ρ^{α} and ρ^{β} have the same free energy.

Using the microscopic description of the wetting phenomenon, one can determine the value of the contact angle θ that is the basis of the macroscopic description. From Eq. 1.1, one has

$$\theta = \frac{\sigma^{sv} - \sigma^{sl}}{\sigma^{lv}}, \tag{2.3}$$

with

$$\sigma^{sv} = \int_0^{+\infty} \Psi^{sv}(y)dy \ , \ \sigma^{sl} = \int_0^{+\infty} \Psi^{sl}(y)dy \quad \text{and} \quad \sigma^{lv} = \int_{-\infty}^{+\infty} \Psi^{lv}(y)dy,$$

where the substrate is assumed to be at $y = 0$. It is worth noting that Ψ^{sv}, Ψ^{sl} and Ψ^{lv} depend on the respective density profiles and thus obey different boundary conditions.

2.2 Wetting of surfaces by complex fluids - Liquid Crystals

In this section we will further present the main characteristics of the wetting by nematics and also the already existing theoretical and experimental results in wetting by cholesterics.

2.2.1 Director and Order parameter tensor

The concept of **director** of a liquid crystal was already introduced in Chapter 1 and is defined as being an unitary vector **n(r,t)** that gives the average of the molecules' orientations within a given volume for a certain time t or, due to ergodicity, the time average of a single molecule's orientation in a certain position **r**. Assuming rod-like molecules, their orientation is defined by a vector **u** aligned along their long axis. The fluctuations of the molecules' orientations **u** in respect to **n** can be quantified by a *scalar order parameter* S, or in other words by a nematic degree of order, which is defined as an average over an ensemble of molecules of the second Legendre polynomial evaluated for the dot product between the molecular orientations **u** and the director **n**: $S = \langle P_2(\cos\theta)\rangle$. One can easily show this if one considers the reference frame where the z-axis is chosen

to be aligned with the director $\mathbf{n}$ and the molecular orientations $\mathbf{u}$ are parameterized as $\mathbf{u} = (\sin(\theta)\cos(\phi), \sin(\theta)\sin(\phi), \cos(\theta))$ (see Fig. 2.4).

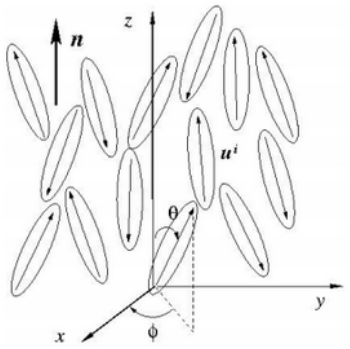

Figure 2.4: Schematic representation of the molecular orientations $\mathbf{u}^i$ and average orientation (given by the director $\mathbf{n}$) and their relation with the parameterization angles. Adapted from Fig.9 in [10].

In this work we are concerned with the study of uniaxial[1] liquid crystals, where all the directions in the plane perpendicular to $\mathbf{n}$ are equivalent. Therefore the orientational distribution function $g(\theta, \phi)$, which gives the probability dP of finding a molecule oriented within a solid angle $d\Omega$ as $dP = (1/4\pi)g(\theta, \phi)d\Omega$, does not depend on the azimuthal angle ϕ – $g(\theta, \phi) \rightarrow g(\theta)$. Thus, $g(\theta)$ can be expanded in terms of the Legendre Polynomials $P_n(\cos\theta)$ as:

$$g(\theta) = \sum_{n=0}^{+\infty} g_n P_n(\cos\theta), \tag{2.4}$$

where the coefficients g_n are given by $g_n = \frac{2n+1}{2}\int_{-1}^{1} g(\theta)P_n(\cos\theta)d(\cos\theta)$.

The first coefficient g_0 of the expansion is constant ($g_0 = 1$) and the odd terms will vanish due to the $\mathbf{n} \longleftrightarrow -\mathbf{n}$ symmetry. Thus the first significant orientation sensitive expansion term will be g_2, which is used to define the scalar order parameter as

$$S = \frac{g_2}{5} = \frac{1}{2}\int_{-1}^{1} g(\theta)P_2(\cos\theta)d(\cos\theta) = \langle P_2(\cos\theta)\rangle, \tag{2.5}$$

where the angle brackets represent the average over the orientational distribution function, i.e., the average over an ensemble of molecules. S can take values in the interval $\left[-\frac{1}{2}, 1\right]$: $S = 1$ corresponds to a perfect nematic with all the molecules exactly aligned with the director, $S = 0$ corresponds to the isotropic state where there isn't a preferential direction of alignment and $S = -1/2$ corresponds to a perfect alignment of the molecules within the plane perpendicular to the director.

Now, one can ask "What is the order parameter that best describes a liquid crystal?". Since liquid crystals possess a center of symmetry, the average of $\mathbf{u}$ vanishes and, therefore,

[1] In uniaxial liquid crystals, there is only one preferred molecular orientation described by the director $\mathbf{n}$.

one can not introduce a vector order parameter, for example the director, analogous to the magnetization in a ferromagnet. One needs to consider higher harmonics in $\mathbf{n}$, i.e., a tensor order parameter. The natural order parameter to describe ordering in uniaxial liquid crystals is the second-rank tensor

$$Q_{\alpha\beta} = \frac{S}{2}\left(3n_\alpha n_\beta - \delta_{\alpha\beta}\right), \tag{2.6}$$

which we call the *tensor order parameter* – S is the scalar order parameter, n_α are the components of the director and $\delta_{\alpha\beta}$ is the kronecker delta. This is a symmetric and traceless tensor. Its largest eigenvalue is the scalar order parameter S and the correspondent eigenvector the director $\mathbf{n}$. In uniaxial liquid crystals the other two eigenvalues are equal since the plane perpendicular to $\mathbf{n}$ is isotropic. $Q_{\alpha\beta}$ describes conveniently the molecular ordering, being zero in the isotropic phase, $Q_{\alpha\beta} = 0 \quad \forall\alpha,\beta$ since $S = 0$, and being sensitive to the direction of the average orientation of the molecules as well as to the orientational distribution of the molecules around their average orientation. $Q_{\alpha\beta}$ also describes complex situations where the nematic ordering varies in space due to the presence of external fields, regions in the LC where the nematic order isn't well defined or in the presence of a nematic-isotropic interface.

2.2.2 Landau - de Gennes Model

Most liquid crystals are either thermotropic or lyotropic, i.e., their liquid crystalline phase is stabilized either for a certain temperature or molecular concentration, respectively. In the present dissertation we are concerned with the thermotropic kind of liquid crystals where the temperature is the main parameter which drives the transition between the isotropic and liquid crystalline phases.

Cholesteric-Isotropic transition

To model the cholesteric-isotropic transition one uses a phenomenological theory which can be constructed independently of the detailed nature of the interactions and of the molecular structure. Since near the transition the tensor order parameter acquires small values, one can use a mean-field Landau-type approach and expand the cholesteric free energy functional in powers of the order parameter $Q_{\alpha\beta}$. The free energy must be invariant under rigid rotations of the axes (x, y, z), so all terms in the expansion must be scalar functions of the order parameter. Thus, we expand the free energy density in terms of the invariants of the tensor order parameter. The simplest free energy volume density needed to model the CI transition is [5]:

$$f_{bulk} = f_0 + \frac{1}{2}a\left(T - T^*_{CI}\right)Q_{\alpha\beta}Q_{\beta\alpha} + \frac{1}{3}BQ_{\alpha\beta}Q_{\beta\gamma}Q_{\gamma\alpha} + \frac{1}{4}C\left(Q_{\alpha\beta}Q_{\beta\alpha}\right)^2, \tag{2.7}$$

where the summation over repeated indices is implied. f_0 is the free energy density of the isotropic phase, which is defined as being zero. a, B and C are the cholesteric material parameters, T is the temperature and T^*_{CI} the supercooling temperature, i.e., the temperature at which the isotropic phase becomes unstable. While B and C are constants, the first term's prefactor $a\,(T - T^*_{CI})$ depends on the temperature hence driving the CI transition. In the unstable isotropic phase regime ($T < T^*_{CI}$), both a and C are positive whereas B is negative, i.e., the prefactors of both first and second terms of the expansion are negative whereas the prefactor of the third term is positive.

The free energy functional that describes the cholesteric degree of order in bulk can be written in terms of the scalar order parameter by introducing the expression (2.6) into the free energy density (2.7). The trace invariants of $Q_{\alpha\beta}$ become $Q_{\alpha\beta}Q_{\beta\alpha} = 3S^2/2$ and $Q_{\alpha\beta}Q_{\beta\gamma}Q_{\gamma\alpha} = 3S^3/4$ leading to the final expression of f_{bulk}:

$$f_{bulk} = \frac{3}{4}a\,(T - T^*_{CI})\,S^2 + \frac{1}{4}BS^3 + \frac{9}{16}CS^4. \tag{2.8}$$

Now that one has f_{bulk} depending only on S, the physical interpretation of the role of the Landau expansion terms becomes straightforward. The first term of the expansion drives the CI transition as it was already said. Fig. 2.5 depicts the temperature dependence of $f_{bulk}(S)$ illustrating the CI transition. When the temperature is higher than the cholesteric-isotropic coexistence temperature T_{CI}, the global minimum of the free energy occurs at $S = 0$ meaning that the isotropic phase is the preferred one. For $T = T_{CI}$, there's a break of symmetry in the system and the cholesteric and isotropic phases become equally stable. At this temperature there can be coexistence of the isotropic and cholesteric phase with a finite amount of order $S = S_{CI}$. The cholesteric-isotropic transition is therefore a *first order phase transtion*. For $T < T_{CI}$, the global minimum of the free energy corresponds to $S \neq 0$ – cholesteric phase. When T equals the supercooling temperature T^*_{CI}, the isotropic phase becomes completely unstable with respect to the cholesteric ordering. The term of the Landau expansion in S^3 introduces a break of symmetry in S, distinguishing the S and $-S$ states. The last term, being positive in the stable cholesteric phase, ensures that the free energy density is bounded from below. It is worth noting that the CI transition is of first order due to the fact that the expansion term of the order S^3 is non-vanishing (S^3's prefactor is constant).

The equilibrium cholesteric degree of order S_{eq} can be determined by minimizing the free energy $F_{bulk} = \int f_{bulk} dV$:

$$S_{eq} = \begin{cases} 0, & T > T_{CI} \\ \frac{1}{2}\left[-B/3C + \sqrt{(B/3C)^2 - 8a(T - T^*_{CI})3C/)}\right], & T < T_{CI} \end{cases} \tag{2.9}$$

The isotropic-cholesteric coexistence temperature T_{CI} is determined by solving $F_{iso}(T_{CI}) =$

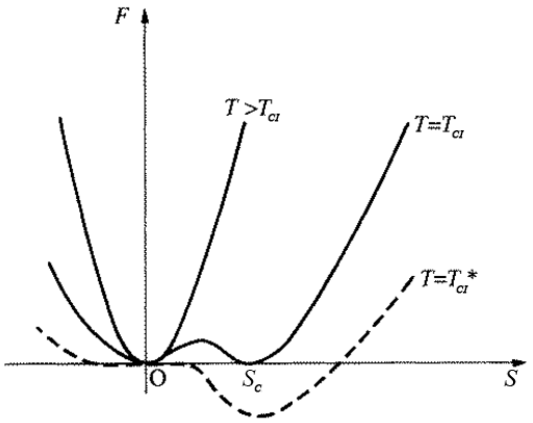

Figure 2.5: Sketch of the cholesteric bulk free energy density as a function of the scalar order parameter S, for different temperature values. For $T = T_{CI}$ there are two minima with the same free energy which correspond to a non-ordered phase ($S = 0$) and an ordered one ($S = S_C$). Adapted from Fig.2.12 in [5].

$F_{Chol}(T_{CI})$ for a non-distorted cholesteric. The detailed calculations can be found in the next Chapter.

Cholesteric elasticity

We already saw that in an ideal nematic liquid crystal, the molecules are on average aligned along a common direction $\pm\mathbf{n}$ and the global ordering can be described by $Q_{\alpha\beta}$. However, in most real scenarios, this ideal ordering is not compatible with constraints imposed by limiting surfaces of the sample (these impose a specific alignment of the molecules) and/or by external fields (electric, magnetic fields, ...). In these cases, there's a deformation of the global alignment characterized by a spacial variation of the order parameter $Q_{\alpha\beta}$. Any orientation deformation can be decomposed in three basic deformation modes: splay, twist and bend, as depicted in Fig. 2.6.

In most situations of interest, significant variations of $Q_{\alpha\beta}$ occur over distances much larger than the molecular dimensions. Therefore, the deformations of the molecular ordering can be described by a continuum theory, disregarding the structure details at the molecular scale, i.e., the deformations can be described by a slowly and smoothly varying director $\mathbf{n}$. Oseen and Frank followed this description, which resulted on the construction of a functional that takes into account the energy cost of such deformations of the LC's ordering. Under these deformations, liquid crystals act as effective elastic materials and thus the energy cost is quantified using elastic constants. Frank introduces the Frank elastic constants which directly characterize each basic deformation: K_1 for splay, K_2 for twist and K_3 for bend. Therefore, the Frank-Oseen elastic free energy density which takes

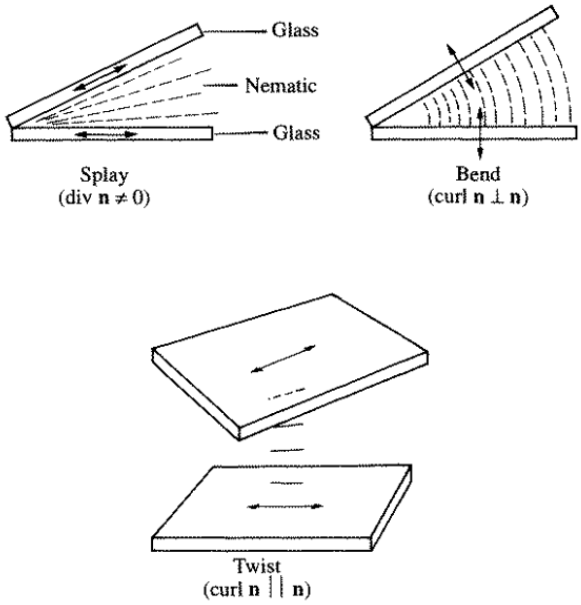

Figure 2.6: Molecular orientations for the three basic elastic deformations. The figure shows how one can obtain these distortions separately by choosing suitable glass walls. Adapted from the Fig.3.1 in [5]

into account the nematic elastic distortions reads as [5]

$$f_{el,N}^{FO} = \frac{1}{2}K_1 \left(\nabla \cdot \mathbf{n}\right)^2 + \frac{1}{2}K_2 \left[\mathbf{n} \cdot (\nabla \times \mathbf{n})\right]^2 + \frac{1}{2}K_3 \left[\mathbf{n} \times (\nabla \times \mathbf{n})\right]^2 . \tag{2.10}$$

In terms of the tensor order parameter, one can construct an elastic free energy functional from the scalar invariants of $Q_{\alpha\beta}$, similarly to what was done for the energy functional that takes into account the CI transition. The common expression for the elastic free energy volume density in terms of $Q_{\alpha\beta}$ has the form [5, 11]:

$$f_{el,N} = \frac{1}{2}L_1 \partial_\gamma Q_{\alpha\beta} \partial_\gamma Q_{\alpha\beta} + \frac{1}{2}L_2 \partial_\beta Q_{\alpha\beta} \partial_\gamma Q_{\alpha\gamma}, \tag{2.11}$$

with L_1 and L_2 being the tensorial elastic constants, ∂_i the derivative in respect to the Cartesian coordinate x_i and where the summation over repeated indices is assumed. These elastic constants are independent of the nematic degree of order. The L_i relate with the Frank elastic constants by:

$$L_1 = \frac{K_3 + 2K_2 - K_1}{9S^2} ,$$
$$L_2 = \frac{4(K_1 - K_2)}{9S^2}.$$

This is the elastic free energy volume density for a nematic. Now, for a cholesteric, which in certain cases can be considered as a stack of nematic layers that rotate along their perpendicular direction, the free energy density also needs to take into account the

natural twist of the cholesteric. This twist is quantified by $q_0 = 2\pi/P_0$, where P_0 is the cholesteric natural periodicity – *pitch*. The formulation for the elastic free energy density of a cholesteric then reads:

$$\begin{aligned} f_{el} &= \frac{1}{2}L_1\left(\epsilon_{\alpha\gamma\delta}\partial_\gamma Q_{\delta\beta} + 2q_0 Q_{\alpha\beta}\right)^2 + \frac{1}{2}L_2\partial_\beta Q_{\alpha\beta}\partial_\gamma Q_{\alpha\gamma} \\ &= \frac{1}{2}L_2\partial_\beta Q_{\alpha\beta}\partial_\gamma Q_{\alpha\gamma} + \frac{1}{2}L_1\left[\partial_\gamma Q_{\alpha\beta}\partial_\gamma Q_{\alpha\beta} + 4q_0\epsilon_{\alpha\beta\gamma}Q_{\alpha\delta}\partial_\beta Q_{\gamma\delta} + (2q_0 Q_{\alpha\beta})^2\right]. \end{aligned} \tag{2.12}$$

Landau-de Gennes Free Energy

Finally, the Landau-de Gennes (LdG) free energy functional, which describes the state of a cholesteric in bulk, is simply the combination of the free energy that describes the cholesteric degree of order in bulk with the free energy that penalizes elastic distortions of the molecular ordering. Therefore, the Landau-de Gennes free energy volume density f_{LdG} reads as:

$$f_{LdG} = f_{bulk} + f_{el}. \tag{2.13}$$

The LdG model is a phenomenological mesoscopic model and, thus, it's the central model for cholesteric liquid crystals at the micro and sub-micron mesoscale, taking into account the spacial variation of the cholesteric degree of order and the cholesteric elasticity. This model applies for arbitrary geometries, different length scales and can be easily modified to incorporate the effects of external fields. However, due to its mean-field nature, it is not suitable for descriptions at the nanoscale – the order parameter tensor, which is the main element of the LdG model, assumes a molecular orientation average over an ensemble of molecules which in turn has a typical length of a few nm. Therefore, detailed descriptions at the nanoscale require molecular approaches, such as *Density Functional Theory*(DFT)-based approaches.

The ratio between the two contributions for the LdG free energy introduces a characteristic length scale, known as the cholesteric correlation length ξ. The correlation length sets the spacial scale for the variation of the degree of order. In nematics and cholesterics its role is more noticeable since ξ determines the size of the nematic/cholesteric defects. Later on we will also see that ξ is the parameter that determines the resolution of the mesh in the numerical calculations.

It is useful to introduce rescaled quantities in order to have a dimensionless free energy. Numerically, this makes it easier to choose the values of the parameters since they come in units of physical quantities. The rescaled quantities are therefore [12, 4]:

$$\begin{gathered} \tilde{Q} = \frac{9C}{2B}Q\ ,\ \tau = \frac{27a(T - T^*_{CI})C}{B^2}\ ,\ \kappa = \frac{L_2}{L_1}\ , \\ \tilde{F} = \frac{3^6 C^3}{\xi^3 B^4} \qquad \text{and} \qquad \tilde{r} = \frac{r}{\xi}, \end{gathered} \tag{2.14}$$

where $\xi^2 = 18C/B^2(3L_1 + 2L_2)$ and $\tilde{Q}$, τ, κ, $\tilde{F}$ and $\tilde{r}$ are the reduced order parameter tensor, reduced temperature, reduced elastic constant, reduced energy and reduced length, respectively. In this formalism, the lengths are in units of correlation length, in particular, the pitch P_0. In terms of these reduced quantities, the rescaled LdG free energy volume density reads:

$$\tilde{f}_{LdG} = \frac{2}{3}\tau\tilde{Q}_{\alpha\beta}\tilde{Q}_{\beta\alpha} - \frac{8}{3}\tilde{Q}_{\alpha\beta}\tilde{Q}_{\beta\gamma}\tilde{Q}_{\gamma\alpha} + \frac{4}{9}\left(\tilde{Q}_{\alpha\beta}\tilde{Q}_{\beta\alpha}\right)^2 + \\ + \frac{1}{3+2\kappa}\left[\tilde{\partial}_\gamma\tilde{Q}_{\alpha\beta}\tilde{\partial}_\gamma\tilde{Q}_{\alpha\beta} + \kappa\tilde{\partial}_\beta\tilde{Q}_{\alpha\beta}\tilde{\partial}_\gamma\tilde{Q}_{\alpha\gamma} + 4\tilde{q}_0\epsilon_{\alpha\beta\gamma}\tilde{Q}_{\alpha\delta}\tilde{\partial}_\beta\tilde{Q}_{\gamma\delta} + (2\tilde{q}_0\tilde{Q}_{\alpha\beta})^2\right]. \tag{2.15}$$

The minus sign $(-)$ in the prefactor of the term in $\tilde{Q}_{\alpha\beta}\tilde{Q}_{\beta\gamma}\tilde{Q}_{\gamma\alpha}$ accounts for B being negative at the stable cholesteric phase.

2.2.3 Surface anchoring

When a liquid crystal is in contact with a solid, liquid or gas, the interface affects the LC ordering imposing a preferred degree of order and molecular orientation. This imposed ordering at the interface is known as *anchoring*. The most frequent types of anchoring are: *homeotropic*, where the LC molecules prefer to align perpendicularly to the interface; *planar*, where the molecules prefer to align along one particular direction parallel to the interface; and *planar degenerate*, where the molecules prefer to lie parallel to the interface with no particular in-plane direction [13].

In this work, the free energy that penalizes deviations from the preferred fixed ordering, homeotropic or planar, at the interface was chosen to be linear in $Q_{\alpha\beta}$ in order to take into account the ordering enhancement near the interface. Therefore, the surface free energy density reads:

$$f_{surf} = -\frac{2}{3}\omega Q_{\alpha\beta}Q^0_{\alpha\beta}, \tag{2.16}$$

where again the summation over repeated indices applies, ω is the surface anchoring strength and $Q^0_{\alpha\beta}$ is the surface-preferred tensor order parameter.

Following the steps of what was done for the LdG free energy, here too one can obtain a dimensionless surface free energy by introducing a rescaled surface anchoring constant [12]:

$$\tilde{\omega} = \frac{36C\omega}{B^2\xi}. \tag{2.17}$$

In terms of the reduced quantities, the dimensionless surface free energy density for the fixed surface anchoring becomes:

$$\tilde{f}_{surf} = -\frac{2}{3}\tilde{\omega}\tilde{Q}_{\alpha\beta}\tilde{Q}^0_{\alpha\beta}. \tag{2.18}$$

2.2.4 Wetting condition

Having introduced the free energy densities which play an important role in interfacial and wetting phenomena, we are in a good position to set the condition under which a substrate is wet by a liquid crystal. In the beginning of the Chapter we introduced wetting phenomena of simple fluids: a substrate is said to be dry when it is contact with the vapor phase and wet when it is contact with the liquid phase. We also said that there are two ways of wetting the system: by decreasing the temperature or by increasing the pressure.

In LC systems the panorama is similar. The difference is that now the substrate is said to be dry when it is in contact with the isotropic phase and wet when a cholesteric film grows between the substrate and the isotropic phase. Here too there are two mechanisms of wetting: by decreasing the temperature or by increasing the strength ω of the preferred anchoring at the substrate (which imposes a certain order, breaking the symmetry of the isotropic phase, and leading to the development of the cholesteric phase). In this work we are interested in the situation in which the wetting transition is driven by the substrate anchoring strength. In order to study the role of ω in wetting phenomena the system has to be at the CI coexistence temperature so that it doesn't favor any of the two phases.

When considering a substrate/wall in contact with the isotropic phase of a LC at the LC-isotropic coexistence temperature, in terms of energy the wall is wet by a LC film when the energy of the wet state equals the energy of the dry state:

$$F_{dry} = F_{wet}. \tag{2.19}$$

Since at coexistence the free energy of the bulk LC and isotropic phases is equal to zero, the free energy of the dry state is in fact the free energy of the interface wall-isotropic phase and the free energy of the wet state is the sum of the free energies of the interfaces wall-LC and LC-isotropic phase. Therefore, the wetting condition becomes

$$F_{wall-isotropic} = F_{wall-LC} + F_{LC-isotropic}. \tag{2.20}$$

This condition is set by the value of the anchoring strength. The value of ω for which the above equation is valid is called the *transition anchoring constant* ω^t. Therefore, one has the wetting transition in a LC system when

$$F_{WI}(\omega^t) = F_{W\ LC}(\omega^t) + F_{LC\ I}. \tag{2.21}$$

2.2.5 Topological defects

When liquid crystals are subjected to confinement, defects in the ordered structure can emerge as a result of opposing preferred molecular orientations at the confining surfaces/interfaces. These defects are, in simple words, regions in the liquid crystal where the

molecules are frustrated and have no preferred orientation. They are generally characterized by a molecular scale core region where there are strong fluctuations of the molecular orientations and by a far field region where the director field changes slowly in space. Therefore, the presence of a topological defect is easily determined from the analysis of the director field on any surface enclosing its core [14].

Defects in nematic liquid crystals, and thus in cholesterics, can be either lines (disclination lines) or points [5]. Using topology one can characterize the defects by assigning a topological invariant to line defects called winding number k and a topological charge q to point defects [14]. Fig. 2.7 shows a schematic view of $\pm 1/2$ disclination lines and ± 1 point defects with the surrounding director field.

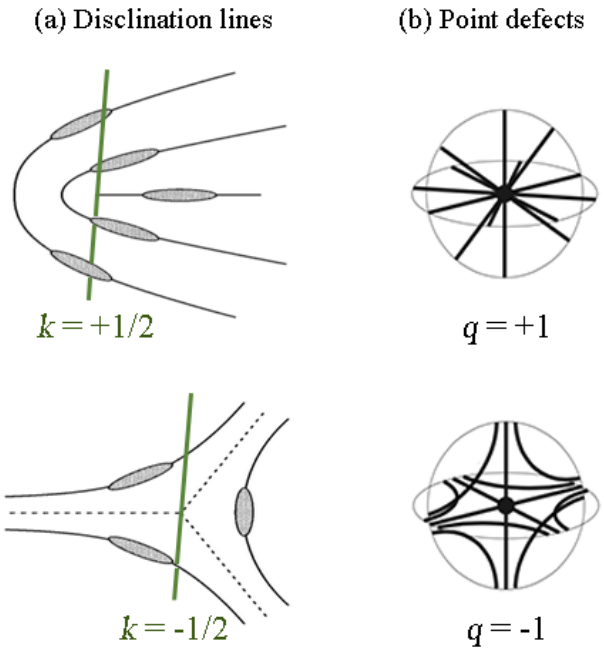

Figure 2.7: Examples of stable disclination lines (left) with half-integer winding number k and stable point defects (right) with integer topological charge q. The disclination line is represented by the green line and the molecules illustrate the director field configuration around the defect. Adapted from Fig.9.2.25 in [14] and from Fig.2.6 in [15].

The winding number, sometimes called the *strength* of the line defect, characterizes the director field around the defect's core, giving the number of times the director rotates along a closed loop surrounding the disclination line. Using topology, the characterization of the defects can be related to topological properties of the order parameter space. For a three-dimensional director field, the order parameter space is simply the surface (S_2) of the unit sphere. The director field along a closed loop Γ surrounding the defect line can be mapped onto the order parameter space provided $\mathbf{n}$ remains unchanged after a complete circuit of Γ [14] (see Fig. 2.8). Due to the symmetry $\mathbf{n} \rightarrow -\mathbf{n}$ the antipodal points of the order parameter space S_2 are identified/equivalent.

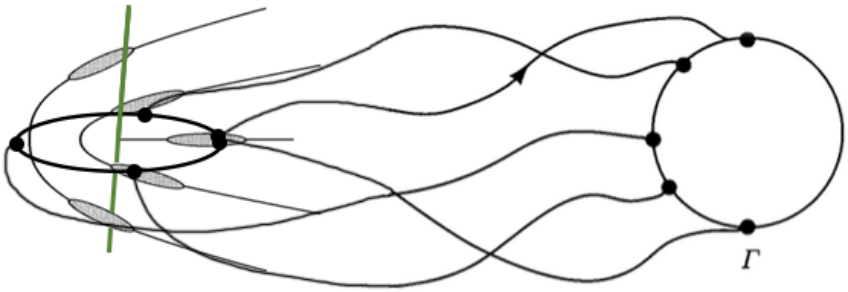

Figure 2.8: Mapping of the distortion of the director field in a closed circuit around a +1/2 defect line into the order parameter space. A +1/2 disclination line corresponds to a non-closed contour in S_2. Adapted from Fig.9.2.24 and Fig.9.2.5 in [14].

Therefore there are two types of contours in S_2 as depicted in Fig. 2.9: (a) a closed contour corresponding to an integer winding number and (b) a non-closed contour terminating at two antipodal points which corresponds to a half-integer winding number.

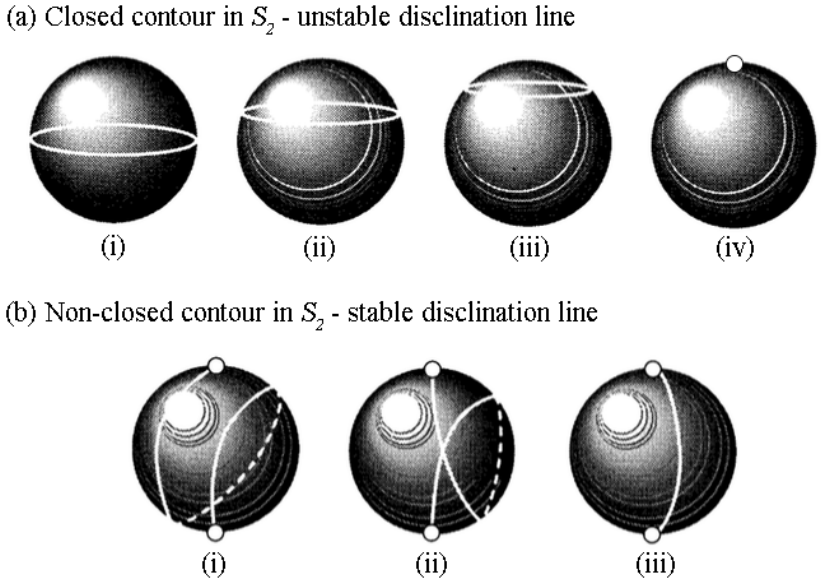

Figure 2.9: Mapping of (a) unstable and (b) stable disclination lines into S_2. (a) i-iv: continuous distortion of an integer line defect into a uniform LC; (b) i-iii: continuous distortion of a $k = 3/2$ to a $k = 1/2$ disclination line. Adapted from Fig.9.1.12 and Fig.9.2.26 in [14].

The closed contour (Fig. 2.9(a)) corresponds to a non-stable line defect since it can be shrunk to a point, i.e., it is topologically equivalent to a uniform director field. On the other hand, the non-closed contour (Fig. 2.9(a)) corresponds to a stable line defect since it cannot be deformed into a point. As one can see from Fig. 2.9(b), all half-integer disclination lines can be smoothly transformed into $+1/2$ or $-1/2$ disclination lines. Therefore, the $\pm 1/2$ disclination lines are the only topologically stable line defects in nematic liquid crystals.

The topological charge q of a point defect is defined as an integral over a closed surface σ surrounding the defect. As in the characterization of line defects, the features of point defects can also be related to the topological properties of S_2: the director field along the enclosing surface σ can be mapped into a surface Σ in S_2 (see Fig. 2.10). If Σ covers S_2 only partially, then it corresponds to an unstable point defect since it can be continuously deformed into a point. The point defect will be topologically equivalent to the uniform field. But if Σ completely covers the unit sphere S_2, then it cannot be contracted to a point hence corresponding to stable defect configurations. The topological charge of the defect is simply the number of times Σ covers the unit sphere S_2 and thus stable point defects correspond to integer values of q.

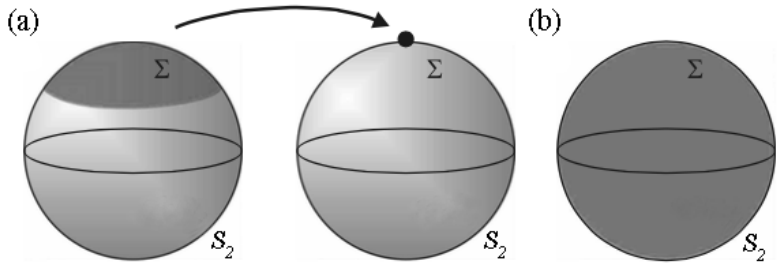

Figure 2.10: Mapping of (a) unstable and (b) stable point defects into S_2. (a) A mapping Σ covering partially S_2 can be continuously distorted to point (uniform LC), corresponding to an unstable defect. (b) A mapping which fully covers S_2 characterizes a stable point defect. Adapted from Fig.2.8 in [15].

The winding number and the defect's charge are topological invariants, having to be preserved when defects are created or annihilated. Since k_{net} and q_{net} is simply the sum of k and q of all the defects, whenever a defect is introduced into a uniform nematic it has to be compensated by a defect of opposite sign. When generated, two defects of opposite signs are attracted to each other until they annihilate, preserving the initial winding number and topological charge.

2.2.6 Wetting of planar surfaces by nematics

Being well acquainted with the nematic bulk properties, let's review the main results of the interfacial phenomena in nematic liquid crystals. We said previously that the nematic-isotropic transition is first order and thus the nematic phase with a finite value of the order parameter can coexist with the isotropic phase with a vanishing order parameter. The study of the properties of the nematic-isotropic (NI) interface is then important when studying nematic systems since one can easily have the formation of a stable NI interface.

The first thing to note is that the free NI interface is always flat, where by free we mean in absence of external constraints. The same isn't true for cholesterics as one shall see further ahead. Since in the absence of external fields the director field is uniform, the

molecular configuration near the NI interface is the same throughout the whole extent of the interface, giving rise to a flat interface.

The preferred anchoring of the molecules at the interface is set by the elastic properties of the liquid crystal, i.e., by the value of κ. Within the Landau-de Gennes free energy, there are only two stable molecular orientations at the NI interface: planar and homeotropic. This can been seen in Fig. 2.11 that presents the surface tension of the NI interface as a function of the anchoring angle α – angle between the director and the interface – for different values of κ.

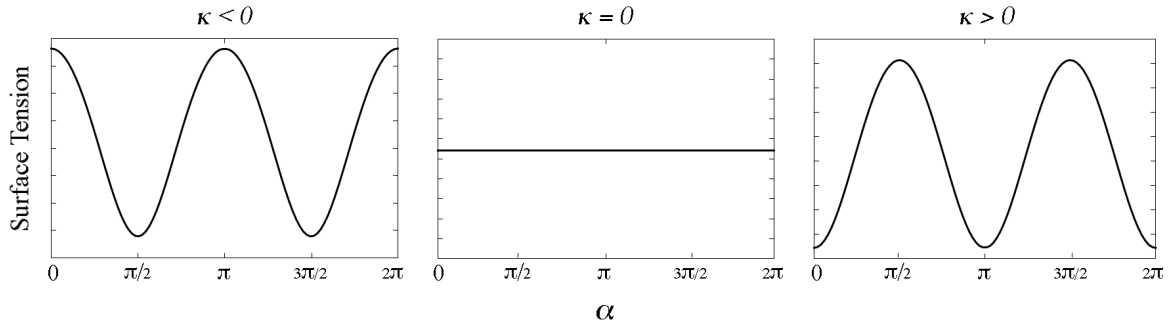

Figure 2.11: Surface tension as a function of the anchoring angle α for (left) $\kappa < 0$, (center) $\kappa = 0$ and (right) $\kappa > 0$.

For $\kappa > 0$, the surface tension is minimum when α equals integer multiples of π (planar anchoring) and for $\kappa < 0$ the surface tension is minimized when α is equal to integer multiples of $\pi/2$ (homeotropic anchoring). At $\kappa = 0$ there isn't a favored ordering at the interface. Thus, if one starts with a nematic configuration whose director field is tilted in respect to the interface at $\kappa \neq 0$, the system will relax to a planar or homeotropic configuration.

In Fig. 2.12 the surface tension is plotted as a function of the reduced elastic constant κ for the two "allowed" molecular orientations at the interface, i.e., for two nematic systems with an uniform director field parallel or perpendicular to the interface.

As expected for $\kappa < 0$ the configuration which minimizes the free energy is the homeotropic one and for $\kappa > 0$ it's the planar configuration. At $\kappa = 0$ both configurations have the same surface tension meaning that both are equally favored. It is also worth noting that the value of the surface tension doesn't depend on κ for the system with a director field perpendicular to the NI interface.

Returning to wetting, the transition anchoring constant ω^t for the uniform nematic can be easily determined for the two configurations where the director field is parallel and homeotropic to the NI interface. Following the studies of Pedro Patrício *et al* in [16] one

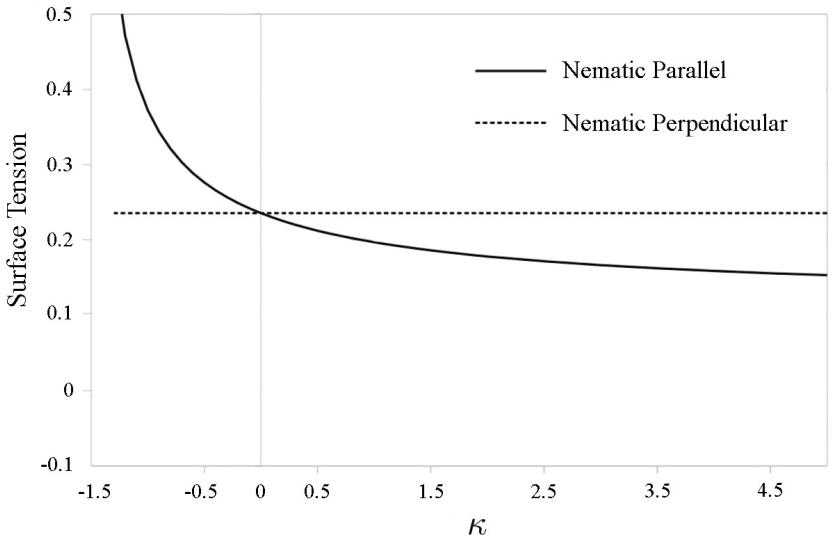

Figure 2.12: Surface tension of the nematic-isotropic interface as a function of κ. The full line curve corresponds to a nematic whose director field is parallel to the NI interface and the dashed line curve corresponds to a perpendicular configuration.

has:

$$\begin{aligned} & F_{WI}(\omega^t) = F_{WN}(\omega^t) + F_{NI} \Leftrightarrow \\ & \Leftrightarrow \omega^t = \sigma^{NI} = \begin{cases} \frac{\sqrt{2}}{6} & \text{, homeotropic} \\ \frac{\sqrt{2}}{6}\sqrt{\frac{6+k}{6+4k}} = \frac{1}{6}\sqrt{\frac{6+k}{3+2k}} & \text{, planar} \end{cases} \end{aligned} \tag{2.22}$$

In other words, the transition anchoring constant is simply given by the surface tension of the NI interface.

2.2.7 Interfacial phenomena in cholesteric systems

In contrast to nematics, interfacial phenomena in cholesteric systems are much more complex. The natural twist of the cholesteric layers introduces a new constrain into the system which leads to additional frustrations of the molecular ordering when the cholesteric is subjected to confinement. Several experimental and theoretical studies show evidence of the formation of complex defect structures near the cholesteric interface [17, 18, 6].

According to the studies in [17], a large pitch cholesteric, when held between two parallel glass plates a distance $d > P$ apart near the CI transition, develops a characteristic striped pattern. The distance between the stripes is found to be about the half pitch $P/2$. If a cholesteric configuration with the twist axis parallel to the plates is assumed, theoretical calculations predict that for homeotropic or planar anchoring of the molecules at the walls/plates there is formation of a lattice of χ disclination lines at the surface of

the sample (Fig. 2.13) [17].

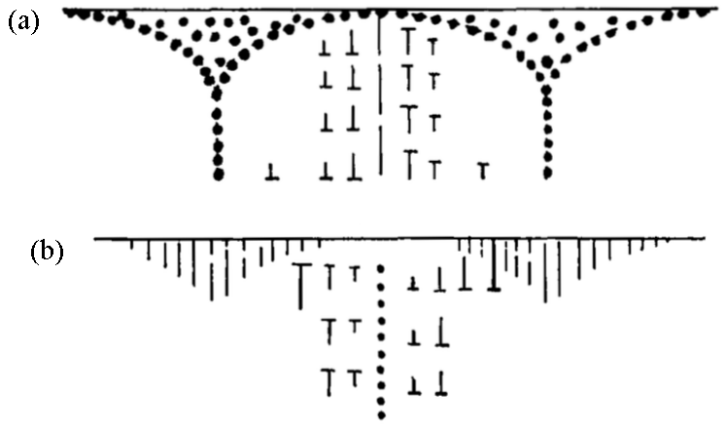

Figure 2.13: Director field near a flat wall favoring (a) parallel or (b) homeotropic anchoring for a cholesteric with the twist axis parallel to the wall. For these configurations there is the formation of singular χ disclination lines at the wall. Adapted from Fig.4 in [17].

As one can see from the schematic representation in Fig. 2.13, the distance between the χ's is about $P/2$. This configuration of χ disclination lines is found to be unstable though, and it is suggested that these singular defects simply split into a singular defect line τ and a non-singular λ line as depicted in Fig. 2.14 [17, 19, 20].

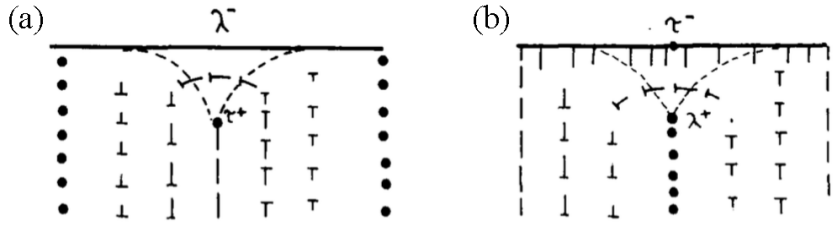

Figure 2.14: Splitting of a χ disclination line into a (a) λ^- and a τ^+ or (b) λ^+ and a τ^- lines when a cholesteric with a twist axis parallel to the wall experiences a favored (a) parallel or (b) homeotropic anchoring. Adapted from Fig.8 in [17].

The minimum distance between a pair of τ and λ disclination lines is $P/4$. These configurations explain the experimentally observed features of the cholesteric domain texture.

One can think of one of the glass plates as being a flat cholesteric-isotropic interface. In this case, these studies allow us to conclude that if the cholesteric-isotropic interface is flat, one should expect the configuration of defects depicted in Fig. 2.14.

Two years latter, Alfred Saupe in [18] investigated the pattern of the disclination lines which form near the surface when the cholesteric twist axis is perpendicular to the plates (see Fig. 2.15).

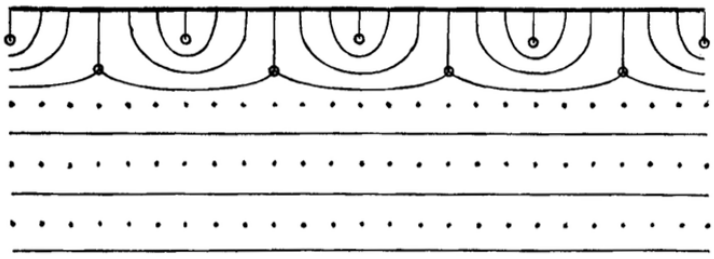

Figure 2.15: Director field near a flat wall favoring homeotropic anchoring for a cholesteric with the twist axis perpendicular to the wall. A lattice of alternating $+1/2$ and $-1/2$ singular disclination lines form at the surface. Adapted from Fig.17 in [18].

When the top surface imposes planar anchoring, the cholesteric remains non-deformed, but when the surface imposes a homeotropic anchoring one has the formation of a lattice of $\tau^{\pm}$ ($\pm 1/2$) disclination lines. Again, if the top surface is considered to be a cholesteric-isotropic interface, this is the expected cholesteric configuration if the CI-interface is flat. R. Meister *et al* in [20] suggested a relaxation of the cholesteric free interface to a waved pattern in order eliminate the energetically cost defect lines.

Rafael Zola *et al* in [6] went further on the study of the cholesteric configuration at the cholesteric-isotropic interface: they studied the pattern formation of a cholesteric under a wetting transition. For this they put the cholesteric in the isotropic phase between two glass plates. At the CI coexistence temperature, a thin LC layer forms at the plates exhibiting a striped pattern (see Fig. 3.1). As the temperature is lowered the wetting layers grow accompanied by a dynamic of the stripes.

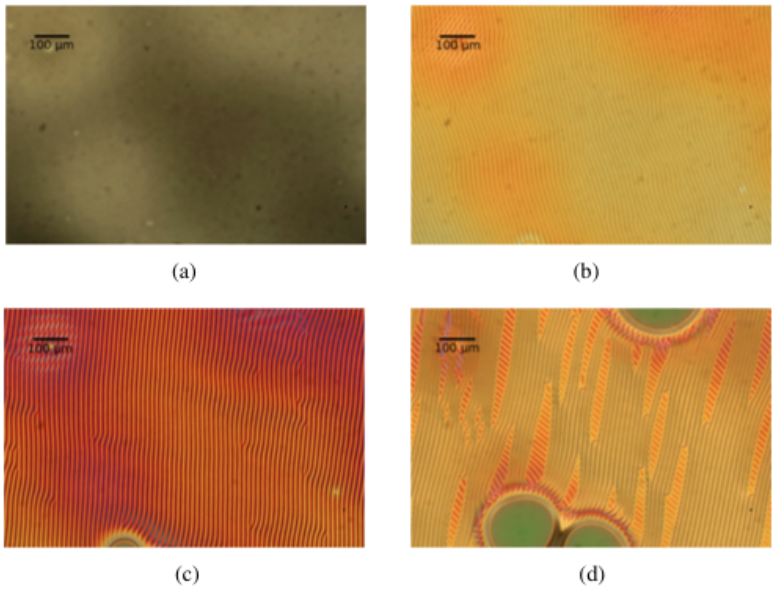

Figure 2.16: Wetting of a planar glass wall by a cholesteric under cooling the sample from the NI coexistence temperature (a) $\rightarrow$ (e). [(b) and (c)] Formation of stripes as the wetting layer grows. (d) Splitting of the stripes. Adapted from Fig.1 in [6].

The study of the system with wetting allows us to have a real CI interface which can relax and evolve to the pattern that minimizes the overall free energy.

Through numerical simulations the authors found the anchoring at the CI interface to be the property responsible for the striped pattern. More specifically, the CI interface configuration is set by the elastic anisotropy and the elastic constant ratios: for certain elastic ratios the striped structure costs too much energy. For other values it can happen that a splay distortion propagates into the bulk and the only way of minimizing this additional cost is the cholesteric being able to undergo an undulated configuration (see Fig. 2.17).

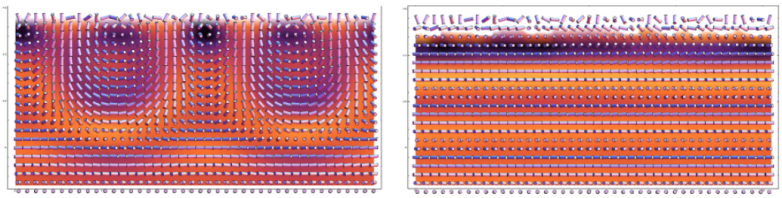

Figure 2.17: Wetting layer for cholesterics with different elastic ratios: (a) $K_1 < 1.6K_2$ and the splay distortion propagates to the bulk. (b) $K_1 > 1.6K_2$ being too energetically expensive to deform the cholesteric layers. Adapted from Fig.4 in [6].

Regarding the cholesteric-isotropic surface tension, A. Rey in [21] studied the role of the pitch P on the CI transition in lyotropic cholesterics: P decreases the critical concentration at witch the CI transition sets in. Although in the present work we are not interested in lyotropic but thermotropic liquid crystals, this results tells us we should expect the parameter which drives the CI transition to depend on P. In other words, the CI coexistence temperature should depend on P.

Chapter 3

Theoretical predictions

In this chapter we present the theoretical predictions for the wetting behavior of a cholesteric in the simplest situation in which there are no elastic distortions of the cholesteric layered structure.

3.1 At the coexistence of the isotropic and cholesteric phases

When considering the isotropic phase of a cholesteric liquid crystal in contact with a substrate, there are several ways to grow a cholesteric film near the substrate. For example, one can start with the isotropic phase at a high temperature in contact with a substrate that imposes a very weak anchoring and then cool the system, or we can start with the isotropic phase at the isotropic-cholesteric coexistence temperature in contact with a substrate and then increase the anchoring strength of the molecules at the substrate. In the former situation, the parameter that drives the wetting transition is the temperature and in the later the parameter is the anchoring strength at the substrate. In this work, we are interested in the study of the wetting transition driven by the anchoring strength of the liquid crystal's molecules at the substrate. This makes wetting phenomena more transparent as it avoids extra complications coming from temperature dependent properties of the liquid crystal. Thus we need to ensure that the system is at the isotropic-cholesteric coexistence temperature. This condition also allows us to study the behavior of the isotropic-cholesteric interface without having a favored phase: the observed effects are the result of interfacial phenomena.

The isotropic-cholesteric coexistence temperature is the temperature at which the bulk cholesteric phase has got the same free energy as the bulk isotropic one. By definition, the free energy of the bulk isotropic phase is zero:

$$Q^{isotropic} = \begin{bmatrix} 0 & 0 & 0 \\ 0 & 0 & 0 \\ 0 & 0 & 0 \end{bmatrix} \Rightarrow F_{LdG}^{isotropic} = \int dV(f_{bulk} + f_{elastic}) = 0. \tag{3.1}$$

Thus, the isotropic-cholesteric coexistence temperature τ^t is the temperature that satisfies

$$F_{LdG}^{cholesteric} = \int dV(f_{bulk} + f_{elastic}) = V\left(\tau S_b^2 - 2S_b^3 + S_b^4 + \frac{1}{3+2\kappa}\frac{3}{2}q_0^2 S_b^2\right) = 0, \tag{3.2}$$

where $S_b = 1/4\left(3 + \sqrt{9 - 4\left(2\tau + 3/(3+2\kappa)q_0^2\right)}\right)$ is the bulk scalar order parameter that minimizes the Landau-de Gennes free energy. Performing the calculation, one obtains

$$\tau^t = 1 - \frac{1}{3+2\kappa}\frac{3}{2}q_0^2. \tag{3.3}$$

This is the isotropic-cholesteric coexistence temperature in the absence of biaxiality. Since the regime of biaxiality is only achieved for very small values of the pitch, this approximation is good enough for our purposes.

The isotropic-cholesteric coexistence temperature depends both on the natural pitch and the reduced elastic constant, in accordance with what was expected from the conclusions drawn in the end of Chapter 2. These are the two parameters whose influence on the cholesteric wetting behavior and interfacial phenomena will be studied.

3.2 Transition anchoring constant for the non-distorted cholesteric

The simplest case of a substrate wet by a cholesteric is the one where there are no elastic distortions of the cholesteric layers. For this situation, one can mathematically model the director field. This allows us to calculate the free energy of the system and ultimately to determine the analytical expression of the transition anchoring constant.

One can achieve this simplest scenario with a substrate that imposes parallel anchoring and by having a favored parallel anchoring of the molecules at the interface ($\kappa \geq 0$), so that one has perfect parallel to the interface and substrate cholesteric layers (Fig.). For such a configuration of the director field, the order parameter tensor is given by

$$Q = \frac{1}{4}S(y)\begin{bmatrix} 1 & 0 & 0 \\ 0 & -2 & 0 \\ 0 & 0 & 1 \end{bmatrix} + \frac{3}{4}S(y)\begin{bmatrix} -\cos(2q_0 y) & 0 & \sin(2q_0 y) \\ 0 & 0 & 0 \\ \sin(2q_0 y) & 0 & \cos(2q_0 y) \end{bmatrix}, \tag{3.4}$$

and, at the isotropic-cholesteric coexistence temperature, the free energy of the system

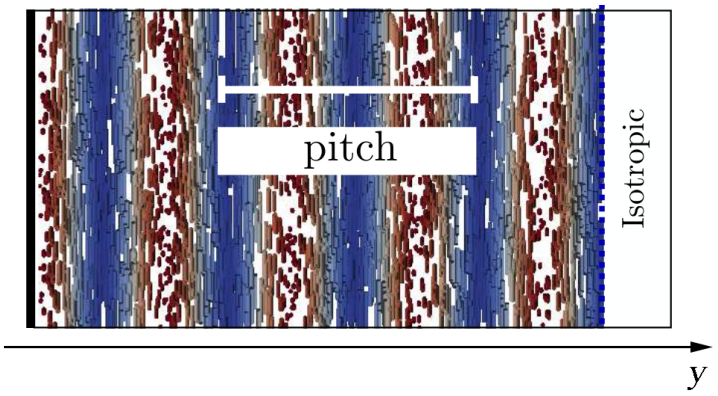

Figure 3.1: Cholesteric configuration for a wall/substrate imposing planar anchoring and for $\kappa \geq 0$. The y-axis gives the direction perpendicular to the CI interface.

becomes

$$F_{LdG}[Q] = L \int dV \left(\tau S(y)^2 - 2S(y)^3 + S(y)^4 + \frac{1}{3+2\kappa}\frac{3}{2}q_0^2 S(y)^2 + \frac{1}{4}\frac{6+\kappa}{3+2\kappa}\frac{\partial S(y)}{\partial y}^2 \right) + \\ + \int dS \left(-\omega S(0)\right). \tag{3.5}$$

Accordingly with what was stated in Section 2.2.4, the condition for having wetting of a substrate/wall by a cholesteric liquid crystal is

$$F_{WI}(\omega^t) = F_{WC}(\omega^t) + F_{CI}(\omega^t), \tag{3.6}$$

where F_{AB} is the free energy of the $A-B$ interface and I, C and W denote the isotropic phase, the cholesteric phase and the substrate/wall, respectively. The transition anchoring constant ω^t is the value of ω that satisfies this condition. To calculate it, first one has to determine the expressions of the free energies.

In order to determine F_{WI} and F_{WC} one considers a substrate in contact with the isotropic and cholesteric phases, respectively. The small variation of the bulk scalar order parameter S_{bulk} near the substrate is described by the ansatz for the scalar order parameter

$$q(y) = S_{bulk} + a_0 e^{-\frac{y}{y_0}}. \tag{3.7}$$

In the isotropic phase $S_{bulk} = 0 \Rightarrow q(y) = a_0 e^{-\frac{y}{y_0}}$ and in the cholesteric phase $S_{bulk} = 1 \Rightarrow q(y) = 1 + a_0 e^{-\frac{y}{y_0}}$. So, at the coexistence and after minimizing the free energy in order to y_0 and a_0, one gets:

$$F_{WI}(\omega) = A\left(-\frac{\omega^2}{2}\sqrt{\frac{3+2\kappa}{6+\kappa}}\right) + \mathcal{O}(\omega^3), \tag{3.8}$$

$$F_{WC}(\omega) = A\left(-\frac{\omega^2}{2}\sqrt{\frac{3+2\kappa}{6+\kappa}} - \omega\right) + \mathcal{O}(\omega^3), \tag{3.9}$$

where A is the area of the system's cross section perpendicular to the twist axis of the cholesteric. Substituting these results in Eq. 3.6, the wetting condition becomes:

$$\omega^t = \frac{1}{A}F_{CI}(\omega^t). \tag{3.10}$$

Finally, to determine F_{CI} one considers a free isotropic-cholesteric interface, with the scalar order parameter varying accordingly with the ansatz $q(y) = \frac{1}{2}(tanh(y/y_0)+1)$. So, at the coexistence and after minimizing the free energy in order to y_0, one obtains:

$$F_{CI} = A\frac{1}{6}\sqrt{\frac{6+\kappa}{3+2\kappa}}. \tag{3.11}$$

Introducing this result in Eq. 3.10, one gets the expression of the transition anchoring constant:

$$\omega^t = \frac{1}{6}\sqrt{\frac{6+\kappa}{3+2\kappa}}. \tag{3.12}$$

ω^t does not depend on the pitch. From this result one sees that the transition anchoring constant for a cholesteric with non-distorted and parallel to the interface cholesteric layers ($\kappa \geq 0$) is the same as the one for a nematic whose director field is also parallel to the isotropic-nematic interface ($\kappa \geq 0$) (See Eq. 2.22 on Section 2.2.6). In other words, when there are no elastic distortions of the cholesteric layers, the cholesteric and the nematic have the same wetting properties. This result was already expected since locally, i.e. at a scale smaller than the pitch, the cholesteric is a nematic (a cholesteric is no more than nematic layers that rotate relatively to each other).

It's important to note that this derivation of the expressions for τ^{CI} and ω^t assumes no biaxiality nor cholesteric distortions. In order to verify the validity of our approximations, on Chapter 5 we perform a numerical determination of τ^{CI} and ω^t and compare both results with the theoretical ones. This way we guarantee that our numerical model is in accordance with what is expected from the theory.

Chapter 4

The Numerical Model

In this chapter the numerical model used to explore the interfacial and wetting properties of cholesterics is explained, in particular the relaxation/minimization methods and the data analysis.

4.1 The system

The cholesteric system taken into consideration in this study is illustrated in Fig. 4.1. For the study of interfacial phenomena the system is composed by a cholesteric in coexistence with the isotropic phase and for the study of wetting properties the cholesteric is held between the CI interface and a surface/wall parallel to the interface.

When we add the CI interface or the wall to the system we break translational symmetry only along the direction perpendicular to them. Thus, the system remains invariant in the planes parallel to both the CI interface and the wall. Here we take advantage of this symmetry and we only consider a two-dimensional system. Experimentally this is equivalent to observing a slice of the system in the plane that contains the direction of broken symmetry.

The systems we are interested in are the ones required to explore the properties of the CI interface and the wetting transition. For the first case we need a system/simulation box with a free stable CI interface. For the second case, as already said in Chapter 2, the wetting condition is $F_{WI}(\omega^t) = F_{WC}(\omega^t) + F_{CI}$. F_{CI} is the free energy of the free stable CI interface. F_{WC} and F_{WI} are the free energies of a system filled with the cholesteric or isotropic phase respectively, at the CI coexistence temperature, in contact with a wall that imposes a certain anchoring. The way of obtaining these three different systems is summarized in Fig. 4.2.

The initial configuration of the system with the free CI interface is always given by a step-function of the order parameter: a bulk cholesteric is put into contact with its isotropic phase. The initial configurations of the systems with a WC or WI interface are also given by a bulk cholesteric or isotropic phase in contact with a wall. The systems are

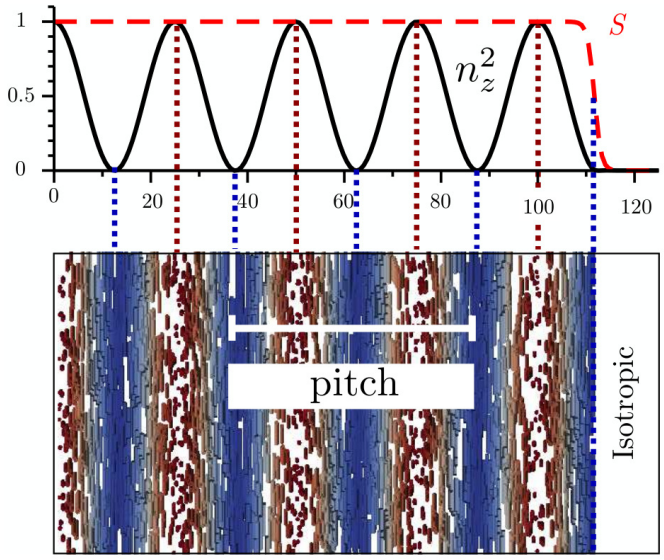

Figure 4.1: Cholesteric-isotropic interface for a cholesteric with planar anchoring and $P = 50\xi$. The rods represent the local average molecular orientations. The color scheme is such that blue rods are aligned in-plane and red rods out-of-plane. The variation of the scalar order parameter S (red line) and the out-of-plane orientation n_z^2 (black line) throughout the system are also plotted. The interface is characterized by an abrupt change in the value of S from $S_b \approx 1$ to $S_b = 0$. Adapted from Fig.1 in [22].

then allowed to relax to their equilibrium configuration. As said in the previous Chapters here we don't follow a molecular approach and thus the equilibrium configuration is found simply by minimizing the free energy functionals which translate the system's thermodynamic behavior. Therefore, the schematic view in Fig.4.1 with the rods is determined a posteriori: we know the value of the components of the order parameter tensor which allows us to infer the components of the local director and hence reconstruct the local average molecular orientation.

The system's representation in Fig. 4.1 is used in the study of the pattern of the CI interface. The color scheme is such that blue rods are align in-plane and red rod point out-of-plane. We label the out-of-plane direction as the z-direction. Fig. 4.1 also shows the variation of the z-component of the director n_z along the system.

The system's representation in Fig. 4.2 is used in the study of the wetting properties. The color scheme goes from red ($S = 0$) to white ($S = S_b = 1$). Again the local director is inferred from the components of the tensor order parameter and the rods show the in-plane orientation and n_z is expressed by the small circumference – the bigger n_z^2 the bigger its radius.

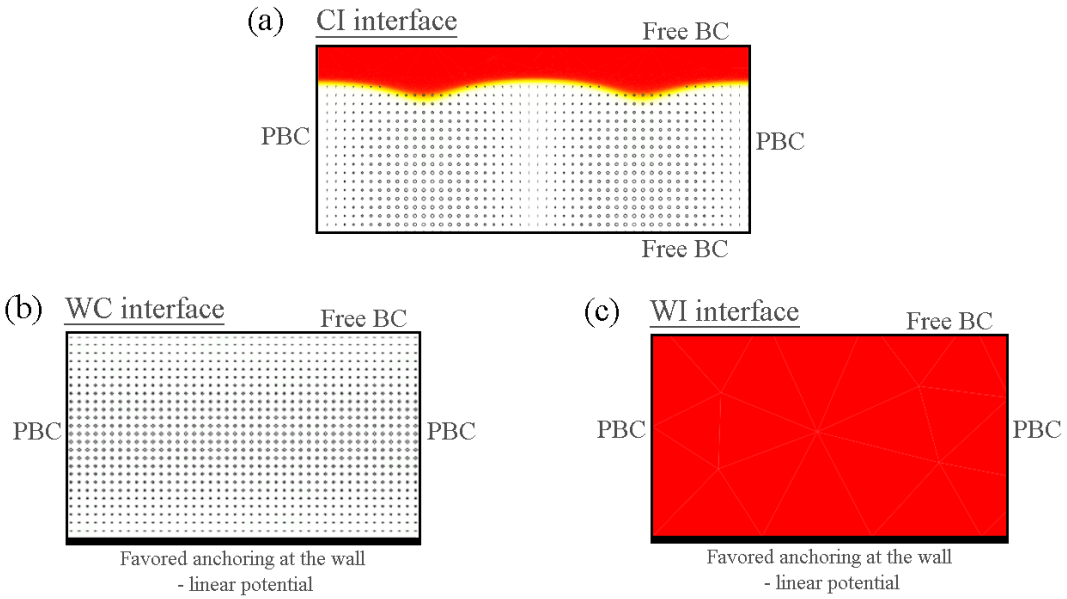

Figure 4.2: Definition of the model systems which allow the determination of the free energy of the (a) CI-, (b) WC- and (c) WI-interfaces. The different boundary conditions (BC) are labeled. PBC stands for Periodic Boundary Conditions. The color scheme goes from red ($S = 0$) to white ($S = S_b = 1$). The local director is also represented: the rods show the in-plane average molecular orientation and the out-of-plane component n_z is expressed by the small circumference – the bigger n_z^2 the bigger its radius.

4.2 Free energy minimization

As said above, the equilibrium configuration of the system is determined by minimizing the energy functional $F_{LdG} = \int f_{LdG} dV$ ($+ \int f_{surf} dS$ when a wall is also considered). This is done using different programs for the different systems in study.

For the study of the properties of the CI interface such as the surface tension and the interfacial pattern the free energy is minimized using a Finite Element Method with a relaxation scheme, through the commercial program COMSOL 3.5a (http://www.comsol.com). The meshes which set the discretization of the system are chosen so that the precision of the numerical results is better than 1%. We use a refined mesh in the region of the CI interface of maximum size ξ in order to obtain a good resolution of the interface. The underlying physics of the system is "given" to the software by setting the *Euler-Lagrange equations*:

$$\partial_\gamma \left(\frac{\partial f}{\partial Q_{\alpha\beta,\gamma}} \right) - \frac{\partial f}{\partial Q_{\alpha\beta}} = 0, \tag{4.1}$$

$$f = f_{LdG} + f_{Lagrange} = f_{LdG} + \mu Q_{\alpha\alpha} + \nu_\alpha \epsilon_{\alpha\beta\gamma} Q_{\beta\gamma}, \tag{4.2}$$

where mu and ν are the Lagrange multipliers which ensure that the tensor $Q_{\alpha\beta}$ is

traceless and symmetric, respectively, and the summation over repeated indices is assumed.

The software solves these equations for the independent components of the order parameter tensor. Having $Q_{\alpha\beta}$ one can determine the configuration of the director field as well as the free energy of the system. The surface tension of the CI-interface, in the case of this two-dimensional system, is just the free energy of the interface per unit length.

For the study of the wetting properties we use a program developed by our research group which has as a Finite Element Method as a basis and minimizes the system's free energy using conjugated gradients. The physics of the system is introduced in the program by setting the free energy densities as functions of the components of the order parameter tensor. The advantage of this program is that it uses adaptive meshes. This way the mesh is more refined in regions where the order parameter is varying, giving a high resolution of the cholesteric configuration near the wall, interface and topological defects, with a less computational cost. The adaptive mesh is refined until a numerical precision of less then 1% is reached.

4.3 Data analysis

Before starting to study the interfacial and wetting properties we need to ensure the system is at the CI coexistence temperature. According to the predictions of Chapter 3, the coexistence temperature depends both on P and κ (see Eq. 3.3). Therefore, the coexistence temperature has to be numerically determined for systems with different sets of values of P and k. The coexistence temperature is determined by changing the temperature of a bulk cholesteric system until its energy equals the energy of a bulk isotropic phase, i.e, equals zero.

After the free energy minimization, the equilibrium free energy of the system comes as an output. So the free energy of the CI interface is immediately obtained, as well as the free energy of the dry state (F_{WI}) and the free energy of the wet state ($F_{WC} + F_{CI}$). In order to find the transition anchoring constant ω^t we calculate F_{WI} and $F_{WC} + F_{CI}$ for several values of ω and the value for which the wetting condition is satisfied is the value of ω^t. For this, we plot the curves $F_{WI}(\omega)$ and $F_{WC}(\omega) + F_{IC}$ and find the value of ω at which these curves intercept, as depicted in Fig. 4.3.

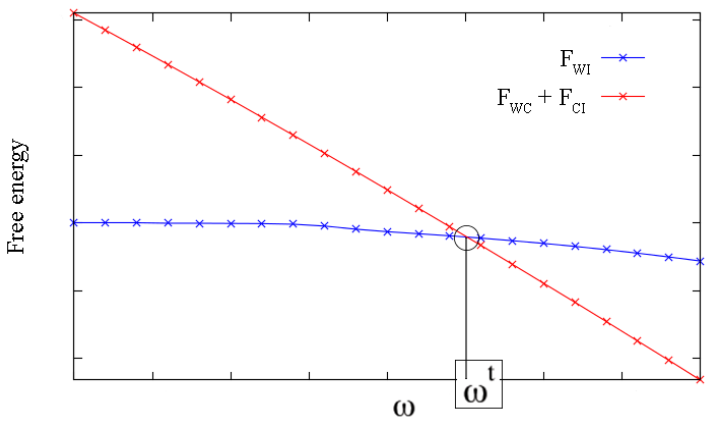

Figure 4.3: Energies crossing method for the determination of the transition anchoring constant ω^t. ω^t is the value for which the wetting condition verifies: $F_{WI}(\omega) = F_{WC}(\omega) + F_{IC}$.

Chapter 5

Cholesteric-Isotropic Interface

In this Chapter we study the fundamental properties of the free isotropic-cholesteric interface using numerical calculations. The pattern of the interface is explored for several values of κ, assuming stable and meta-stable configurations of the interface. We also study the role of the pitch and of κ on both the surface tension and the distortions of the interface.

5.1 The pattern of the interface

On Chapter 2 it was said that, within the used Landau-de Gennes model, there's only two types of anchoring of the LC molecules at the interface: planar and homeotropic. It was also said that $\kappa > 0$ favors the planar anchoring and $\kappa < 0$ the homeotropic one, with $\kappa = 0$ not favoring any.

The easiest way to begin the study of the pattern of the isotropic-cholesteric interface is to start by considering the configuration shown in the Fig. 4.1 for $\kappa > 0$. In this case, the layered structure of the cholesteric phase remains undeformed with the cholesteric layers parallel to the interface. The isotropic-cholesteric surface tension for this case was already calculated in Chapter 3 leading to an expression that was exactly the same as the one for an isotropic-nematic interface – σ_{CI} doesn't depend on the pitch. This result was also confirmed through numerical calculations.

Therefore, the interesting case is the one in which the cholesteric layers are perpendicular to the isotropic-cholesteric interface (see Fig. 5.1 for $P = 1000\xi$). To obtain the configurations in Fig. 5.1(b), we took advantage of the fact that this system has two different relaxation times: the interface relaxes faster than the bulk phase. So, we start with the configuration of Fig. 5.1(a) and then we let the system relax only enough time to have a complete relaxation of the interface but not of the bulk. This way, we can obtain the configuration of Fig. 5.1(b) for $\kappa > 0$, even though it is a meta-stable configuration – when $P = 1000\xi$ the equilibrium configuration for $\kappa > 0$ is the one with the cholesteric layers parallel to the interface. We will see at the end of this Section that this isn't always

true. In fact, the value of k for which there's not a preferential anchoring depends on P, being strictly zero only when $P \to \infty$ [22].

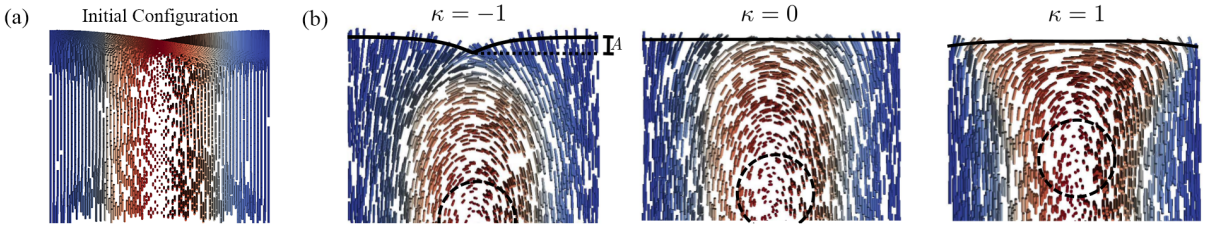

Figure 5.1: Configuration of the CI interface for a cholesteric with $P = 1000\xi$. (a) Set-up of the interface before the minimization as a step-function of the order parameter. (b) Equilibrium configurations for $\kappa = -1$ (left), $\kappa = 0$ (middle) and $\kappa = 1$ (right). The molecular orientation at the interface goes from mostly homeotropic ($\kappa = -1$) to mostly planar ($\kappa = 1$). The full black line gives the position of the interface at $S = S_b/2$ and the dashed black line marks the non-singular λ^+ disclination line. The amplitude A of the interfacial undulations is defined as the difference between the maximum and the minimum of the line $S = S_b/2$. The lateral size of each configuration is $P/2 = 500\xi$. Adapted from Fig.2 in [22].

In this scenario with a layered structure perpendicular to the interface, no matter the anchoring at the interface (planar or homeotropic), there is an intrinsic frustration of the director field which results on the formation of topological defects [7]. In order to avoid the defects, the interface relaxes to a waved pattern so that the equilibrium configuration includes both undulations of the interface and non-singular topological defects (λ^+ disclination lines). These non-singular defects are indicated in Fig. 5.1(b) by the dashed circumferences. Both the period of the interface undulated pattern and the distance between the interface and the non-singular defects are related with the pitch by $P_0/2$ and $P_0/4$, respectively, as predicted by previous theoretical studies [7]. Since there are only two types of anchoring at the interface and for $\kappa = 0$ none of them is favored (when $P = 1000\xi$), the configuration of the interface for $\kappa = 0$ shows equally sized regions of planar and homeotropic anchoring of the molecules at the interface. For negative κ ($\kappa = -1$) the molecules tend to align perpendicularly to interface, violating the preferred anchoring only in small regions. For positive κ ($\kappa = 1$) one has the opposite scenario, where the molecules try to align parallel to the interface in a bigger region.

For very large values of κ, which favors a strong planar anchoring at the interface, the system satisfies the anchoring requirements by breaking the symmetry of the director field near the interface (see Fig. 5.2). Now the period of the pattern near the interface is equal to one pitch instead of half of the pitch. It is important to emphasize that these configurations for $\kappa > 0$ are meta-stable. However, they are of interesting analysis because not only in the experiments meta-stable configurations are often observed but also these configurations are related to some that have been described before [7] [18].

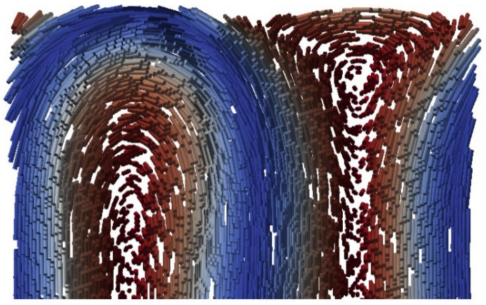

Figure 5.2: Configuration of the CI interface for a cholesteric with $P = 1000\xi$ and $\kappa = 5$. There's a breaking of symmetry and the period of the interfacial pattern becomes a full pitch P. This configuration is meta-stable.

As was said before, the value of κ for which there's not a favored anchoring at the interface depends on the pitch. In Fig. 5.3 one can see this dependence as well as the favored anchoring in the different regions of the parameter space (κ,P). For $P < 42\xi$ we couldn't find a value of κ above which the planar anchoring is favored, suggesting that for the highly twisted cholesteric phase the only stable configuration is similar to the one in Fig. 5.1(b) for $\kappa = -1$. The boundary between planar and homeotropic anchoring lies at $\kappa = 0$ only in the nematic limit ($P \to \infty$). Nevertheless for $P \geq 1000\xi$ this boundary lies at $\kappa \sim 0$, which supports the approximation made in the previous analysis when one stated that the stable cholesteric configuration for $P = 1000\xi$ and $\kappa > 0$ is the one with the cholesteric layers parallel to the interface.

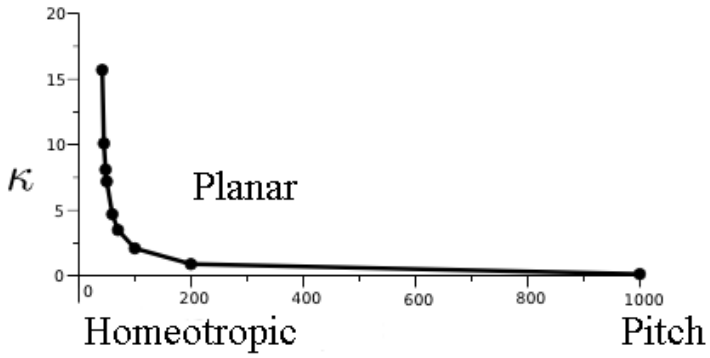

Figure 5.3: Phase diagram for the favored anchoring at the CI interface ($T = T_{CI}$). When $P > 1000\xi$, $\kappa \sim 0$ showing that the nematic behavior is recovered for large values of the pitch. For $P < 42\xi$ a value of κ, above which the the favored anchoring goes from homeotropic to planar, was not found.

5.2 Surface tension

When studying the surface tension, the first thing one needs to clarify is the definition of what is the isotropic-cholesteric interface. Due to the complex elastic distortions, this

definition becomes subtle. There are two, apparently opposed, points of view. In the first one, which can be regarded as a microscopic point of view, the scalar order parameter S changes at the interface over a distance comparable to the bulk correlation length. So if $P >> \xi$ the isotropic-cholesteric interface is similar to the isotropic-nematic interface. From this point of view, the isotropic-cholesteric interface does not include the interface undulations neither the distortions of the cholesteric layers and, thus, these should not be taken into account when calculating the surface tension. The second point of view is a macroscopic or thermodynamic one. At a macroscopic scale, the isotropic-cholesteric interface is effectively flat. The amplitude of the undulations is much smaller than the pitch. So, for a cholesteric with a pitch in the micron scale, the undulations are most likely bellow the visible wavelengths, which makes the interface appear flat when observed with an optical microscope. Also, from a thermodynamic view point, the surface tension is the free energy cost of increasing the area of an interface. Thus, if one doubles the area of the interface, one must double the distortions. This implies that the energetic cost of the distortions must be included in the surface tension. Hence, the interface undulations and the distortions of the cholesteric layers are part of the isotropic-cholesteric interface. Therefore, the definition of the interface and of the surface tension depends on the length scale at which one studies the system. We are interested in the thermodynamic surface tension so we will follow the latter point of view.

We want to understand the role of the two important parameters P and κ on the behavior of the surface tension. Hence we calculated the surface tension of configurations such as those of Fig. 5.1 for different values of P and κ. The obtained results for the surface tension are summed in Fig. 5.4.

Looking at Fig. 5.4(a), that shows the dependence of the surface tension on κ, one sees that in a cholesteric with $P = 1000\xi$ the effect of the undulations and distortions of the cholesteric layers on the surface tension is small. For $\kappa > 0$ the values of the surface tension for an isotropic-cholesteric interface match the ones for an isotropic-nematic interface, although the cholesteric configuration is not the stable one – one already said that the stable configuration for $\kappa > 0$ is the one with cholesteric layers parallel to the interface. For $\kappa < 0$ there are deviations from the surface tension of the nematic, but these deviations are of small magnitude given the increase of the surface tension due to the undulations and distortions of the cholesteric layers. If one looks now to a cholesteric with $P = 20\xi$, we observe a completely different behavior of the surface tension. The value of the surface tension deviates from the surface tension of the nematic, decreasing as we go towards more negative values of κ. It even becomes negative at $\kappa \approx -0.5$ meaning that in this region of the parameters the cholesteric phase is no longer the thermodynamic stable one. This is a signature of the presence of stable blue phases in the phase diagram [22]: we observe stable blue phases for $\kappa < 0.593$. The strong decrease of the surface tension for negative values of κ is due to the formation of regions of double-twist that have lower energy than

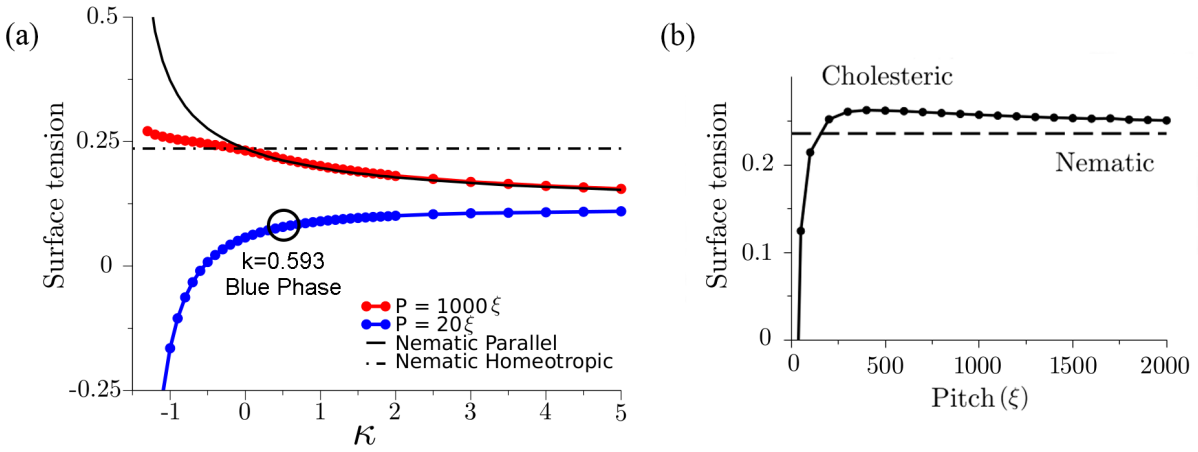

Figure 5.4: CI interface's surface tension as a function of (a) κ and (b) the pitch for a cholesteric the layers perpendicular to the interface. (a) Surface tension as a function of κ for a cholesteric with $P = 1000\xi$ (red) and $P = 20\xi$ (blue). The black curves are results for the NI interface's surface tension for a nematic with planar (full line) and homeotropic (dashed line) anchoring at the interface. Note that the surface tension for $P = 20\xi$ decreases with the decrease of κ, contrary to what happens for $P = 1000\xi$, becoming even negative for $\kappa \lesssim -0.5$. This suggests the cholesteric phase is no longer thermodynamically stable in this region of parameters. We observe the formation of a blue phase for $\kappa < 0.593$. (b) Surface tension as a function of P for a cholesteric with $\kappa = -1$. The dashed line corresponds to the NI surface tension for a nematic with homeotropic anchoring at the interface. The CI surface tension reaches a value close to the nematic's for $P > 200\xi$ and decreases slowly for high values of the pitch towards the NI surface tension with homeotropic anchoring. Adapted from Fig.3 in [22].

the bulk cholesteric phase. It is worth noting that these exotic phases are only found around the transition from the isotropic to the cholesteric phase. If we were not at the CI coexistence, but instead at a lower temperature, the cholesteric phase would be perfectly stable [23]. From the results shown in Fig. 5.4(a) one can also conclude that there are two regimes with respect to the surface tension's behavior: the one for big P in which it approaches the surface tension of the nematic and the one for small P in which there is a strong decrease of the surface tension for more negative values of κ.

Looking now to Fig. 5.4(b), that shows the dependence of the surface tension on P for $\kappa = -1$, one can clearly distinguish the two different regimes. For $P < 200\xi$ one sees the strong dependence of the surface tension on the value of P which reflects the formation of regions of double-twist and the proximity to blue phases in the phase diagram. For $P > 200\xi$ the result approaches the asymptotic value for the nematic. In the latter regime, the difference between the surface tension for the cholesteric and for the nematic is due to the undulations and distortions of the cholesteric layers.

5.3 Interface's undulations

One can also study the influence of κ and P on the undulations of the interface. The undulations' amplitude A was measured as being the difference between the heights of the maximum and minimum of the isoline $S = S_b/2$ as shown in Fig. 5.1. The results of the calculation of the amplitude are presented in Fig. 5.5.

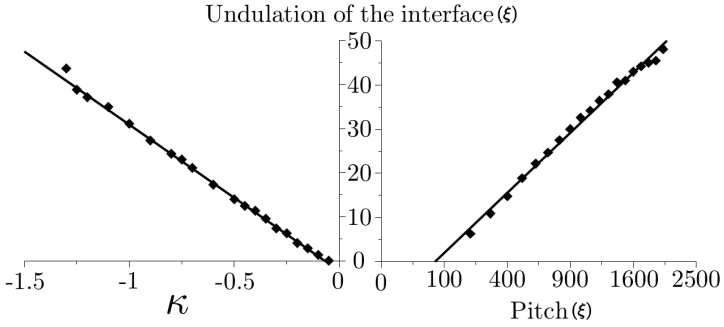

Figure 5.5: Amplitude of the undulations of the CI interface (a) as a function of κ for a cholesteric with $P = 1000\xi$ and (b) as a function of P for a cholesteric with $\kappa = -1$. The results were obtained for a cholesteric with layers perpendicular to the interface. The full lines are linear fits to the results: (a) $A = -33.1\kappa - 2.2$ and (b) $A = 1.359\sqrt{P} - 11.6$. Adapted from Fig.4 in [22].

On the left, the amplitude is plotted as a function of κ for a cholesteric with $P = 1000\xi$. For positive κ the stable configuration is the one with the cholesteric layers parallel to the interface and so there are no undulations. Hence the amplitude is only plotted for negative values of κ. For negative κ we see that the amplitude linearly varies with $|\kappa|$. This behavior was also observed for other values of the pitch, $P > 200\xi$. On the right side of Fig. 5.5, the amplitude is plotted as a function of $\sqrt{P}$ for $\kappa = -1$. The amplitude is also linear in $\sqrt{P}$. Therefore, in the nematic limit ($P \to \infty$) the ratio A/P goes to zero, as expected. We observed the same quantitative behavior for other negative values of κ.

The linear dependence of the undulations' amplitude on $|\kappa|$ ($\kappa < 0$) and $\sqrt{P}$ does not have a trivial explanation since the undulations result from a complex interplay between the cholesteric elastic distortions, the surface tension and the anchoring at the interface. Using the ansatz of Ref. [7], the calculations of the free energy of an interface that may change its configuration at a fixed director configuration lead to the predictions $A \sim P$ and $A \sim \kappa^2$ [22]. Comparing the configurations that result from this ansatz with our results, one concludes that the ansatz fails due to the inaccurate description of the liquid crystal configuration near the interface. The fact that the scaling $A \sim P$ breaks down is a clear sign of the presence of two length scales in the system: P and ξ. Even though in general $\xi << P$, the influence of ξ is important since the interface undergoes an undulated pattern to avoid the formation of additional topological defects whose size and position are determined by ξ. The scaling of A with κ and P is set by the minimization of the

elastic distortions while avoiding the formation of these additional topological defects. We haven't been able to perform this minimization analytically.

Chapter 6

Cholesteric Wetting

In this section we show, as a result of numerical calculations, how a cholesteric wets a planar surface that imposes parallel anchoring of the LC molecules. As it was said previously, the study of the wetting properties is done in terms of the transition anchoring constant. Here we analyze the role of P and κ on the behavior of ω^t. We start by presenting the results for the simplest case of wetting where the are no distortions of the cholesteric film's layers and then we will proceed to the more interesting case in which elastic distortions deform the cholesteric layered structure.

6.1 The simplest system: "non-distorted" Cholesteric

In Chapter 3 the wetting behavior of a cholesteric with $\kappa > 0$ in contact with a substrate that imposes parallel anchoring was determined through theoretical calculations. In this case, the I-C interface favors parallel anchoring which leads to a non-deformed cholesteric layered structure with the cholesteric layers parallel to the substrate and interface. For this system, the transition anchoring constant has the same expression as the one for a nematic with the director field parallel to the substrate and I-N interface. In this Section we numerically calculate the transition anchoring constant for this simple system to ascertain the validity of the used ansatz in the theoretical calculations. The results are presented in Fig. 6.1.

The numerical results are in accordance with the theoretically predicted ones for the nematic with an error less than 4%. In other words, the used ansatz for the theoretical determination of the transition anchoring constant is supported by the numerical results, within the numerical accuracy. From here one can conclude that, in the "non-distorted" case, the cholesteric and the nematic have the same wetting properties: the anchoring at the substrate for which the wetting transition occurs only depends on κ, i.e., the elastic properties of the cholesteric dictate the wetting behavior.

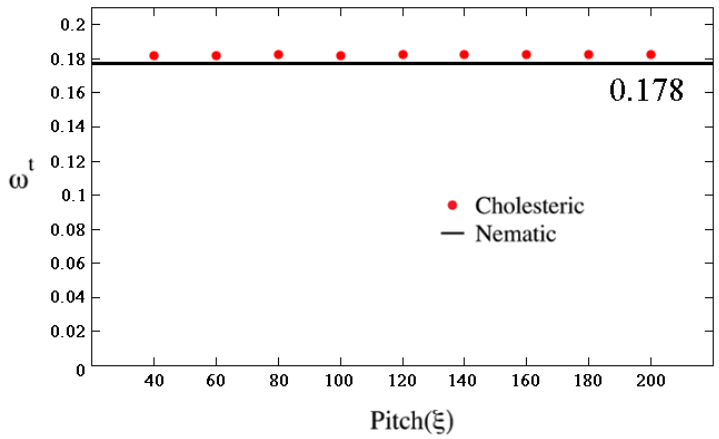

Figure 6.1: Transition anchoring constant ω^t as a function of the pitch for a cholesteric with layers parallel to the substrate/wall and to the CI interface ($\kappa = 2$). The full black line is the result for the nematic with planar anchoring at the substrate and at the NI interface for $\kappa = 2$.

6.2 Facing distorted cholesteric layers

The interesting case when studying the wetting properties of a cholesteric is when there are elastic deformations of the cholesteric layered structure. In Chapter 5 we saw that the equilibrium configuration of the I-C interface for negative values of κ exhibits both undulations of the interface and distortions of the cholesteric layers that are perpendicularly aligned to the interface. Thus, for $\kappa < 0$, the equilibrium configuration of a cholesteric film confined between the I-C interface and a substrate that imposes a strong parallel anchoring will contain additional topological defects (disclination lines) as depicted in Fig. 6.2.

The first thing to do when studying the wetting behavior of a cholesteric under these conditions is to know what is the wet state at the wetting transition: does the cholesteric film first form the additional disclination lines and then the substrate becomes wet or does the cholesteric first wet the substrate and only then there's formation of the topological defects? In order to see if the wet state at the wetting transition contains the additional disclination lines, we numerically determined the value of the anchoring constant at the substrate for which the free energies of the systems with and without the additional defects are equal – ω^* – (see Fig. 6.3).

We started with a system filled with the cholesteric phase in contact with a substrate that imposes parallel anchoring (at the bottom of the system). The cholesteric layers were set to be perpendicularly aligned to the substrate by imposing a fixed anchoring at the top of the system. We increased the value of ω at the substrate until the disclination lines were formed. The energies of the configurations without defects for the different values of ω are plotted in the red curve in Fig. 6.3. After the formation of the defects, we decreased the value of ω, obtaining the blue curve in Fig. 6.3. The crossing point

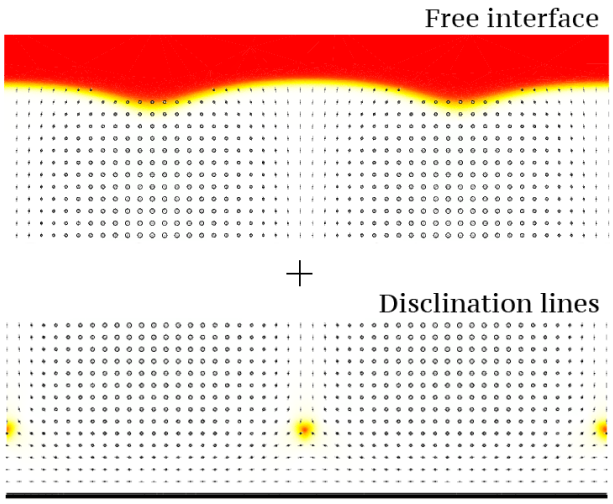

Figure 6.2: Cholesteric configuration of the wet state. The free energy of the wet state is $F_{WC} + F_{CI}$. The WC-interface's free energy comes from the favored anchoring at the wall (surface linear potential). The CI-interface's has got two contributions that come from the variation of the order parameter at the interface along with the elastic distortions of the interface in the form of undulations and from the disclination lines that form near the wall.

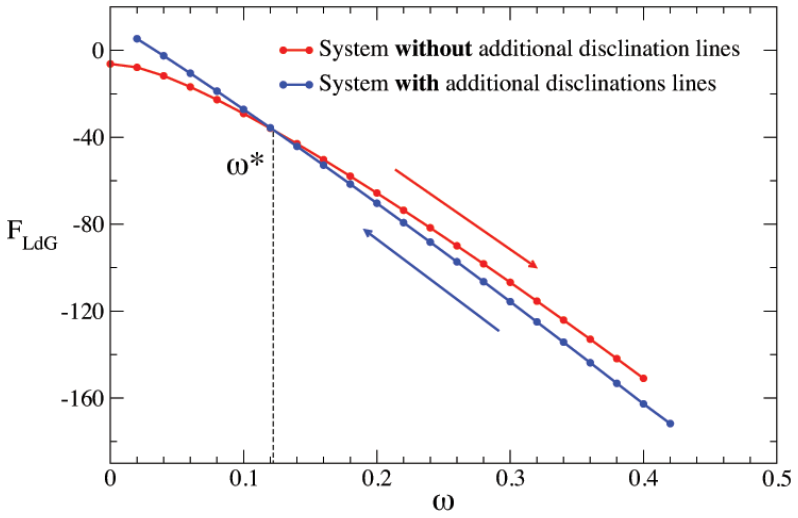

Figure 6.3: Determination of ω^* – value of the anchoring constant for which the cholesteric film configurations with and without disclination lines are equally stable. The plotted results are for a cholesteric with $P = 400$ and $\kappa = -0.5$ (favored homeotropic anchoring at the CI-interface) for a substrate/wall that favors planar anchoring. For this cholesteric system $\omega^* = 0.124$ and $\omega^t = 0.270 \Rightarrow \omega^* < \omega^t =$, meaning that the configuration of the wet state will include disclination lines: as the anchoring strength increases at the wall, first there's the formation of singular disclination lines and then the complete wetting occurs.

of the red and blue curves gives the value of ω^*. Then, we numerically calculated the transition anchoring constant ω^t considering that the wet state at the wetting transition included the additional defects and we obtained that $\omega^* < \omega^t$, i.e., the formation of the

additional defects requires a value of ω that is smaller than the one needed to wet the system. Thus, when increasing ω, first there is the formation of the disclination lines and then the wetting transition occurs. Hence, the wet state at the wetting transition contains the additional disclination lines. Now we are able to correctly determine ω^t for different values of P and κ.

In Fig. 6.4, ω^t is plotted as a function of P for a negative value of κ ($\kappa = -0.5$). The black full line is the result for the nematic with the director field perpendicularly aligned to the I-N interface. The red dots are the values of ω^t for a cholesteric with cholesteric layers perpendicularly aligned both to the I-C interface and the subatrate. The behavior of the transition anchoring constant is very similar to the one of the surface tension for $\kappa < 0$ shown with Fig. 5.4(b)).

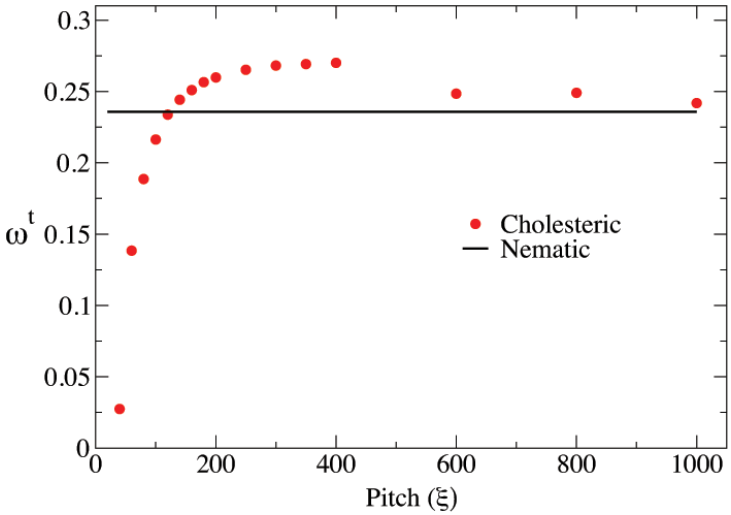

Figure 6.4: Transition anchoring constant ω^t as a function of the pitch for a cholesteric with $\kappa = -0.5$ (favored homeotropic anchoring at the CI-interface) and a substrate that favors planar anchoring. The full black line is the result for a nematic with $\kappa = -0.5$ and thus aligned perpendicularly to the NI-interface. For values of the pitch $> 400\xi$, ω^t decreases towards the nematic result.

One can easily distinguish two regimes: the one for small values of P ($P \leq 400\xi$) and the one for large values of P ($P > 400\xi$). In the former regime, ω^t decreases with the decrease of P. The cause of this behavior is the same as the one for the surface tension: it is due to the formation of double-twist regions that have lower energy than the bulk cholesteric phase. Since these double-twist regions have lower energy, a smaller value of ω is needed to have wetting of the substrate. In the later regime, ω^t approaches the asymptotic regime as we move towards larger values of P. The curve for the cholesteric will eventually converge into the curve for the nematic, but this convergence is very slow. The difference between the values of the cholesteric and nematic curves is due to the undulations of the isotropic-choesteric interface, distortions of the cholesteric layers and also to formation of topological defects near the substrate in the cholesteric systems that

contribute with an additional energetic cost.

Let's now explore the role of κ on the behavior of ω^t taking into account the two different regimes. In Fig. 6.5 and Fig. 6.6, ω^t is plotted as a function of κ for the small pitch regime ($P = 200\xi$) and for the large pitch regime ($P = 400\xi$), respectively. The black full line is the theoretical result for the nematic with the director field perpendicularly aligned to the I-N interface and to the substrate and the black dashed line is the theoretical result for the nematic with the director field aligned parallel to the interface and substrate. The red and blue dots are the numerically calculated values of ω^t for a cholesteric configuration with the layered structure perpendicular and parallel to the I-C interface and substrate, respectively. In both Fig. 6.5 and Fig. 6.6, we see that the blue dots follow the dashed line for the nematic, as expected. When the cholesteric layered structure is parallel to the I-C interface and to the substrate there are no distortions of the cholesteric layers. Hence, as we said previously, the cholesteric follows the wetting behavior of the nematic.

Paying attention to the numerical results of ω^t for a cholesteric with a layered structure perpendicularly aligned to the I-C interface and to the substrate, we see that for the small pitch regime (Fig. 6.5) ω^t decreases as κ decreases. The behavior of ω^t is similar as the one of the surface tension for small values of the pitch (see Fig. 5.4(a)). Again, this behavior is due to the formation of double-twist regions for more negative values of κ. The region of small values of P and more negative values of κ in the parameter space is very propitious to the formation of these double-twist regions.

If we now look to the large pitch regime (Fig. 6.6), we observe a completely different behavior: ω^t is approximately constant and it seems to follow the behavior of the nematic line for a director field perpendicularly aligned to the I-N interface. The difference between the values of ω^t for the cholesteric and for the nematic is due to the elastic energy of the undulations of the I-C interface, distortions of the cholesteric layers and of the additional disclination lines. Here we can also find a similarity between the behavior of ω^t (red dots) and the one for the surface tension in the large pitch regime (see Fig. 5.4(a)). Even though the surface tension for $P = 1000\xi$ deviates from the surface tension of the nematic for $\kappa < 0$, its value stays close to the surface tension of the nematic with the director field perpendicularly aligned to the I-N interface.

In both Fig. 6.5 and Fig. 6.6, the curves of ω^t for the cholesteric (red and blue dots) cross at a negative value of κ, whereas the curves for the nematic cross at $\kappa = 0$ since for this value of κ there is no preferred anchoring at the I-N interface. This deviation of the crossing point from $\kappa = 0$ is due to the fact that the wet state for the cholesteric contains undulations of the I-C interface, distortions of the cholesteric layers and additional disclination lines near the substrate.

From the analysis of the plots of ω^t as a function of P and κ we conclude that ω^t follows the behavior of the surface tension. Hence, one can say that the surface tension drives the wetting transition.

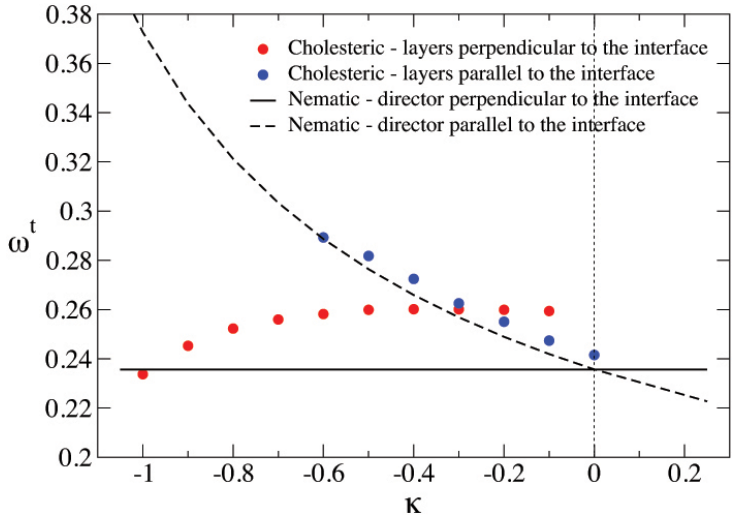

Figure 6.5: Transition anchoring constant ω^t as a function of κ for a cholesteric with $P = 200\xi$ for the two cases where the cholesteric layers are parallel to the substrate and the CI-interface (blue dots) or parallel to the substrate but perpendicular to the interface (red dots). In the second case there are additional disclination lines where the layers with different orientations meet. The black lines are the results for the nematic aligned parallel (dashed line) and perpendicularly (full line) to the NI-interface. ω^t for the red dotted curve decreases with the decrease of κ. This is the same behavior of the CI surface tension for small values of the pitch when the cholesteric layers are perpendicular to the interface. The blue dotted curve follows the nematic curve suggesting that the cholesteric with layers parallel to the substrate and to the CI-interface and the nematic aligned parallel to the substrate and to the NI-interface have the same wetting properties. Note that the curves for the cholesteric cross at $\kappa < 0$, contrary to the nematic ($\kappa = 0$).

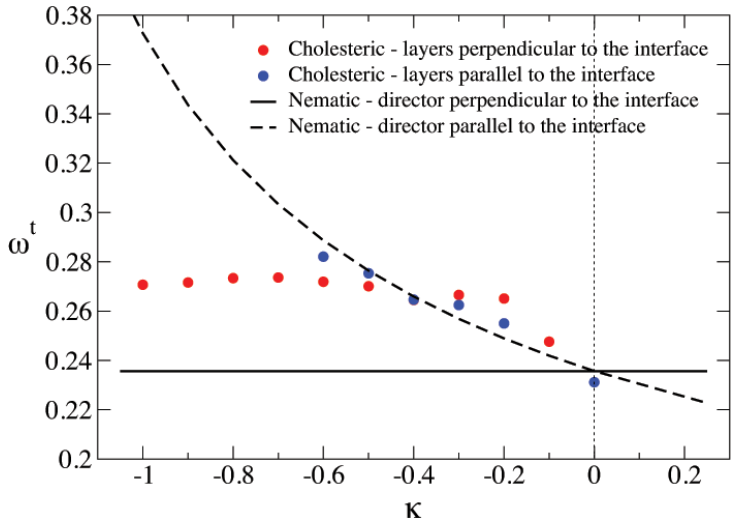

Figure 6.6: Transition anchoring constant ω^t as a function of κ for a cholesteric with $P = 400\xi$. This is the same graphic as the one in Fig. 6.5 but for a different value of the pitch. The difference here is that the value of ω^t for a cholesteric with layers perpendicular to the CI-interface is approximately constant, following the curve for the nematic perpendicularly aligned to the NI-interfce.

Chapter 7

Final Remarks

This thesis is focused on the numerical modeling of a cholesteric-isotropic interface in the absence (free CI interface) and in the presence of a flat substrate/wall. The first case allows us to study the CI interface properties, such as the surface tension and pattern of the interface, and the second case allows us to predict the wetting properties of cholesterics, i.e., the cholesteric configuration near the wall and the CI interface and the role of the cholesteric intrinsic parameters on the wetting transition. The motivation for this work comes from the gaps in the fundamental physics of cholesteric liquid crystals and also from our collaborator's experiments which show a peculiar dynamics of topological defects at the CI interface under wetting of a planar substrate.

We start from the simplest wetting scenario, where both the substrate and the CI interface favor a planar anchoring of the LC molecules. Therefore the cholesteric layers remain parallel to both the substrate and the CI interface without elastic distortions. In such a system it is easy to build an analytic model of the cholesteric configuration since it resembles a stack of nematic layers which rotate along the direction perpendicular to the layers. By constructing the tensor order parameter and using the Landau-de Gennes (LdG) model we are able to calculate the CI interface surface tension. In this work we are concerned with the wetting transition driven by the anchoring strength of the imposed anchoring at the substrate. With this analytic model we are also able to determine the dependence of the transition anchoring constant ω^t – value of the anchoring strength at which the wetting transition occurs – on the cholesteric intrinsic parameters, namely the *pitch* P and the *reduced elastic constant* κ. We find the value of the CI surface tension σ and the transition anchoring constant ω^t to be independent of the cholesteric pitch. Therefore we can say that a non-distorted cholesteric and a nematic have the same interfacial and wetting properties.

Next we head to more complex systems where opposing preferred molecular orientations at the cholesteric bulk and at the confining surfaces (CI interface and substrate/wall) lead to distortions of the cholesteric layers and formation of topological defects. In these systems the CI interface minimizes the high energetic cost of the formation of singular

topological defects near the interface by relaxing to an undulated pattern. We find the amplitude of the interface undulations to scale as $A \sim \sqrt{P}$ and $A \sim k$, contrary to what was suggested in [7]. This shows the presence of two length scales in the system: the pitch P and the correlation length ξ which sets the size and position of the topological defects. Although $\xi << P$, the influence of ξ is still notorious since the interface relaxes to an undulated pattern to avoid the formation of additional topological defects.

Looking at the interface from a macroscopic or thermodynamic point of view the distortions and additional topological defects are part of the interface. By numerically minimizing the system's LdG free energy we can calculate the surface tension and the transition anchoring constant and see how these quantities change with the variation of P and κ. For small values of P, σ and ω^t decrease with the decrease of κ meaning that the cholesteric phase is no longer the thermodynamic stable one. For small values of P and κ we even observe the formation of more exotic phases – blue phases. For large values of P, both quantities approach the asymptotic nematic limit, in accordance with what's expected. The slight difference in the value of σ and ω^t for cholesterics and nematics is due to the presence of the additional topological defects in cholesterics.

From the analysis of the behavior of σ and ω^t as functions of the cholesteric intrinsic parameters we see that ω^t follows the behavior of σ. In other words we conclude that the surface tension drives the wetting transition.

As a closing remark, I'd like to point out that in the past couple of years I had the opportunity to work in an original research project carried out in a research group with a long time experience in the field of the physics of Liquid Crystals. This experience allowed me to work on the development of a numerical model under the supervision of great professionals, which has certainly shaped and matured my skills in the world of scientific research. Our collaboration with an experimentalist group also allowed me to compare our numerical results with real systems, which made me to be more aware of the need to relate theoretial/numerical descriptions to the experimental findinds by trying to create simple models that provide clear descriptions of the underlying physics.

To conclude, the fascination for cholesteric liquid crystals that launched this project led to original and scientific relevant scientific discoveries on this major and active field of the physics of Liquid Crystals. This project contributed to my personal and scientific enrichment and also allowed me to learn how to work as part of a research group.

Bibliography

[1] P. G. de Gennes. *Capillarity and Wetting Phenomena: Drops, Bubbles, Pearls, Waves*. 2004.

[2] D. Bonn et al. Wetting and spreading. *Reviews of Modern Physics*, 81:739, 2009.

[3] J. S. Rowlinson and B. Widom. *Molecular Theory of Capillarity*. 2002.

[4] P. Patrício, J. M. Romero-Enrique, N. M. Silvestre, N. R. Bernardino, and M. M. Telo da Gama. Complex fluids at complex surfaces: simply complicated? *Molecular Physics*, 109:1067, 2011.

[5] P. G. de Gennes and J. Prost. *The Physics of Liquid Crystals*. 1995.

[6] R. S. Zola, L. R. Evangelista, Y.-C Yang, and D.-K. Yang. Surface induced phase separation and pattern formation at the isotropic interface in chiral nematic liquid crystals. *Physical Review Letters*, 110, 2013.

[7] R. Meister, H. Dumoulin, M.-A. Hallé, and P. Pieranski. The anchoring of a cholesteric liquid crystal at the free surface. *Journal de Physique II France*, 6:827–844, 1996.

[8] J. S. Lintuvuori, A. C. Pawsey, K. Stratford, M. E. Cates, P. S. Clegg, and D. Marenduzzo. Colloidal templating at a cholesteric-oil interface: Assembly guided by an array of disclination lines. *Physical Review Letters*, 110, 2013.

[9] Y. Geng, D. Seč, P. L. Almeida, O. D. Lavrentovich, S. Žumer, and M. H. Godinho. Liquid crystal necklaces: cholesteric drops threaded by thin cellulose fibres. *Soft Matter*, 9:7928–7933, 2013.

[10] D. Andrienko. Introduction to liquid crystals. *International Max Planck Research School - Modelling of soft matter*, 2006.

[11] P. G. de Gennes. Short range order effects in the isotropic phase of nematics and cholesteric. *Molecular Crystals and Liquid Crystals*, 12:193, 1971.

[12] N. M. Silvestre, Z. Eskandari, P. Patrício, J. M. Romero-Enrique, and M. M. Telo da Gama. Nematic wetting and filling of crenelated surfaces. *Physical Review E*, 86, 2012.

[13] J.-B. Fournier and P. Galatola. Modeling planar degenerate wetting and anchoring in nematic liquid crystals. *Europhysics Letters*, 72:403–409, 2005.

[14] P. M. Chaikin and T. C. Lubensky. *Principles of condensed matter physics*. 1995.

[15] Miha Ravnik. *Colloidal Structures Confined to Thin Nematic Layers*. PhD thesis, University of Ljubljana, 2009.

[16] P. Patrício, C. T. Pham, and J. M. Romero-Enrique. Wetting transition of a nematic liquid crystal on a periodic wedge-structured substrate. *The European Physical Journal E*, 26:97, 2008.

[17] P. E. Cladis and M. Kléman. The cholesteric domain texture. *Molecular Crystals and Liquid Crystals*, 16:1, 1972.

[18] A. Saupe. Disclinations and properties of the director field in nematic and cholesteric liquid crystals. *Molecular Crystals and Liquid Crystals*, 21:211–238, 1973.

[19] H.-S. Kitzerow and C. Bahr. *Chirality in Liquid Crystals*. 2001.

[20] R. Meister, M.-A. Hallé, H. Dumoulin, and P. Pieranski. Structure of the cholesteric focal conic domains at the free surface. *Physical Review E*, 54:3771, 1996.

[21] A. Rey. Pitch contributions to the cholesteric-isotropic interfacial tension. *Macromolecules*, 33:9468–9470, 2000.

[22] N. R. Bernardino, M. C. F. Pereira, N. M. Silvestre, and M. M. Telo da Gama. Structure of the cholesteric-isotropic interface. *Soft Matter*, 10:9399–9402, 2014.

[23] D. C. Wright and N. D. Mermin. Crystalline liquids: the blue phase. *Reviews of Modern Physics*, 61:385, 1989.